Application of Naturalistic Truck Driving Data to Analyze and Improve Car Following Models

Bryan James Higgs

Thesis submitted to the faculty of the Virginia Polytechnic Institute and State University
in partial fulfillment of the requirements for the degree of

Master of Science
In
Civil Engineering

Montasir M. Abbas
Alejandra Medina
Feng Guo

December 2nd, 2011
Blacksburg, Virginia

Keywords: Naturalistic Data, Car Following, Wiedemann Model, GHR Model,

Using Naturalistic Truck Driving Data to Analyze and Improve Car Following Models

Bryan James Higgs

ABSTRACT

This research effort aims to compare car-following models when the models are calibrated to individual drivers with the naturalistic data. The models used are the GHR, Gipps, Intelligent Driver, Velocity Difference, Wiedemann, and the Fritzsche model. This research effort also analyzes the Wiedemann car-following model using car-following periods that occur at different speeds. The Wiedemann car-following model uses thresholds to define the different regimes in car following. Some of these thresholds use a speed parameter, but others rely solely upon the difference in speed between the subject vehicle and the lead vehicle. This research effort also reconstructs the Wiedemann car-following model for truck driver behavior using the Naturalistic Truck Driving Study's (NTDS) conducted by Virginia Tech Transportation Institute. This Naturalistic data was collected by equipping 9 trucks with various sensors and a data acquisition system. This research effort also combines the Wiedemann car-following model with the GHR car-following model for trucks using The Naturalistic Truck Driving Study's (NTDS) data.

DEDICATIONS

I would like to dedicate this work to all those that have supported me in my ambitions. I would also like to thank everyone for investing their time in me which has made me into the person that I am today. Most of all, I would like to dedicate this work to my late mother. Her influence in my life is irreplaceable and I would not be where I am today without her memory to guide me through life.

ACKNOWLEDGMENTS

This material is based upon work supported by the Federal Highway Administration under Agreement No. DTFH61-09-H-00007. Any opinions, findings, and conclusions or recommendations expressed in this publication are those of the Author(s) and do not necessarily reflect the view of the Federal Highway Administration.
The authors would like to express thanks to individuals at Virginia Tech and the Virginia Tech Transportation Institute who contributed to the study in various ways: Greg Fitch, Shane McLaughlin, Zain Adam, Brian Daily, and Rebecca Olson.

TABLE OF CONTENTS

LIST OF FIGURES

LIST OF TABLES

1. INTRODUCTION

In the last 50 years, a considerable amount of research has focused on modeling longitudinal driver behavior, producing a large number of car-following models including: Gazis-Herman-Rothery (GHR) models, safety distance models, linear models and psycho-physical or action point models. Calibrating these car-following models requires different levels of effort and the results are dependent upon data availability and the calibration method.

Several studies have tried to incorporate driver behavior or to classify driver's attributes, however, direct correlation with real driving variables is rare and parameterization of objective behavior is still in its development. Some studies have been limited to very controlled experiments while recent ones have used aerial photographs based on measurement from helicopters, GPS data, test track data and trajectory data from NGSIM.

As opposed to traditional epidemiological and experimental / empirical approaches, this *in situ* process uses drivers who operate vehicles that have been equipped with specialized sensors along with processing and recording equipment. In effect, the vehicle becomes the data collection device. The drivers operate and interact with these vehicles during their normal driving routines while the data collection equipment is continuously recording numerous items of interest during the entire driving. Naturalistic data collection methods require a sophisticated network of sensor, processing, and recording systems. This system provides a diverse collection of both on-road driving and driver (participant, non-driving) data, including measures such as driver input and performance (e.g., lane position, headway, etc.), four camera video views, and driver activity data. This information may be supplemented by subjective data, such as questionnaire data.

As part of the NTDS study, one hundred drivers were recruited from four different trucking fleets across seven terminals and one to three trucks at each trucking fleet were instrumented (nine trucks total). After a participant finished 4 consecutive weeks of data collection, another participant started driving the instrumented truck. Three forms of data were collected by the NTDS DAS: video, dynamic performance, and audio. Approximately 14,500 driving-data hours covering 735,000 miles traveled were collected.

The following is a typical description of how the data collection is performed, along with accompanying screen shots and information describing how the system works and how data can be used. Four cameras monitor and record the driver's face, forward road view, and left- and right-side of the tractor trailer, which are used to observe the traffic actions of other vehicles around the vehicle. The sensor data associated with the project were originally collected in a proprietary binary file format. A database schema was devised and the necessary tables were created. The schema preserves the organization of data into modules; i.e., all of the variables associated with a particular module are stored in one table in the database.

The Naturalistic Data offers a new insight into driver behaviors. In order to capitalize on this new insight, current car following models need to be evaluated using this data. This evaluation will also reveal areas that could be improved for the car following models.

1.1. Research Objectives

The objectives of this research effort are as follows:

- To compare car-following models when the models are calibrated to individual drivers with the naturalistic data.
- To analyze the Wiedemann car-following model using car-following periods that occur at different speeds.
- To reconstruct the Wiedemann car-following model for truck driver behavior using the Naturalistic Data
- To combine the Wiedemann car-following model with the GHR car-following model for trucks using the Naturalistic Data

1.2. Thesis Contribution

The Naturalistic Data is very detailed and offers a new angle to view driver behavior and thus presents a big opportunity for improving the current state-of-practice. This thesis aims to identify and improve current car following models using the Naturalistic Data.

1.3. Thesis Organization

This thesis consists of six chapters. Chapter 1 presents an introduction and the research objectives. Chapter 2 presents a comparison of car following models when they are calibrated to individual drivers using the Naturalistic Data. Chapter 3 presents an analysis of the Wiedemann model over different speeds. Chapter 4 presents a reconstruction of the Wiedemann model for truck driver behaviors. Chapter 5 presents a combination of the GHR and Wiedemann car following models. Chapter 6 presents the thesis conclusions and future recommendations.

2. COMPARISON OF CAR-FOLLOWING MODELS WHEN CALIBRATED TO INDIVIDUAL DRIVERS USING NATURALISTIC DATA[1]

Abstract
This research effort aims to compare car-following models when the models are calibrated to individual drivers with the naturalistic data. The data used for this research is from the Naturalistic Truck Driving Study conducted by Virginia Tech Transportation Institute. The models used are the GHR, Gipps, Intelligent Driver, Velocity Difference, Wiedemann, and the Fritzsche model. The calibration of each model used 100 car following periods of four different drivers. The results show that some of the models can accurately mimic the behavior of one or two of the drivers, but the error increases for the other drivers. The Wiedemann model and the Velocity Difference model both showed consistency in performance across the four drivers. The results of this research provide clarity into which microscopic traffic flow models can accurately represent the behavior of a variety of drivers.

[1] Paper has been published in the proceedings of the 2011 Transportation Research Board meeting in Washington, D.C.

[2] Paper accepted for presentation at the 3rd International Conference on Road Safety and Simulation

2.1 Naturalistic Driving Data

As opposed to traditional epidemiological and experimental / empirical approaches, this *in situ* process uses drivers who operate vehicles that have been equipped with specialized sensors along with processing and recording equipment. In effect, the vehicle becomes the data collection device. The drivers operate and interact with these vehicles during their normal driving routines while the data collection equipment is continuously recording numerous items of interest during the entire driving. Naturalistic data collection methods require a sophisticated network of sensor, processing, and recording systems. This system provides a diverse collection of both on-road driving and driver (participant, non-driving) data, including measures such as driver input and performance (e.g., lane position, headway, etc.), four camera video views, and driver activity data. This information may be supplemented by subjective data, such as questionnaire data.

As part of the NTDS study [1], one hundred drivers were recruited from four different trucking fleets across seven terminals and one to three trucks at each trucking fleet were instrumented (nine trucks total). After a participant finished 4 consecutive weeks of data collection, another participant started driving the instrumented truck. Three forms of data were collected by the NTDS DAS: video, dynamic performance, and audio. Approximately 14,500 driving-data hours covering 735,000 miles traveled were collected.

The following is a typical description of how the data collection is performed, along with accompanying screen shots and information describing how the system works and how data can be used. Four cameras monitor and record the driver's face, forward road view, and left- and right-side of the tractor trailer, which are used to observe the traffic actions of other vehicles around the vehicle. The sensor data associated with the project were originally collected in a proprietary binary file format. A database schema was devised and the necessary tables were created. The schema preserves the organization of data into modules; i.e., all of the variables associated with a particular module are stored in one table in the database.

2.2 Synthesis of past efforts

Much research effort has been directed at modeling the behavior of drivers. However, direct correlation with real driving variables is rare and parameterization of objective behavior is still in its development. Some studies have been limited to very controlled experiments; recent studies have used aerial photography based measurement from helicopters [2], GPS data, test track data and trajectory data form NGSIM .

Ossen and Hoogendoorn [3] studied the car-following behavior of individual drivers using vehicle trajectory data that were extracted from high-resolution digital images collected at a high frequency from a helicopter. The analysis was performed by estimating the parameters of different specifications of the GHR car-following rule for individual drivers. In 80 % of the cases, a statistical relation between stimuli and response could be established. The Gipps (a safe distance model) and Tampere (stimulus-response model) models and a synthetic data based approach were used for assessing the impact of measurement errors on calibration results. According to the authors, the main contribution of their study was that considerable differences between the car-following behaviors of individual drivers were identified that can be expressed in terms of different optimal parameters and also as different car-following models that appear to be optimal based on the individual driver data. This is an important result taking into account that in most models a single car-following rule is used. The authors also proposed for future research to apply more advanced statistical methods and to use larger databases. Brackstone [4] used data collected with an instrumented vehicle that was assembled at Transportation Research Group at Southampton parameterize the Wiedemann's threshold for a typical following spiral. As a result they represent the action points as a function of a probability distribution based on ground speed.

Micro-simulation software packages use a variety of car-following models including Gipps' (AIMSUN, SISTM, and DRACULA), Wiedemann's (VISSIM), Pitt's (CORSIM), and Fritzsche's (PARAMICS). And different automated calibration parameters such as genetic algorithms have been used to calibrate the distribution of car-following sensitivity parameters *[5]*. Panwai and Dia [6] compared the car-following models between different simulation software, including AIMSUN, PARAMICS and VISSIM using an instrumented vehicle to record differences in speed and headway (Leading speed, relative distance, relative speed, follower acceleration were recorded). The EM shows similar values for psychophysical models in VISSIM and PARAMICS and lower values in AIMSUN. The RMS error and qualitative drift and goal-seeking analyses also showed a substantially different car-following behavior for PARAMICS. Siuhi and Kaseko [7] demonstrated the need for separate models for acceleration and deceleration responses by developing a family of car-following models and addressing the shortcomings of the General Motors (GM) model. Previous work from Osaki [8] and Subranmanian [9] modified the GM model separating the acceleration and deceleration responses. Ahmed [10], following some work from Subranmanian assumed non linearity in the stimulus term and introduced traffic density. Results from Ahmed [10] and Toledo [11] showed , against popular belief, that acceleration increases with speed but decreases with vehicle separation. Due to statistical insignificance, Ahmed and Toledo also removed speed from their deceleration models. Siuhi and Kasvo [7] addressed some of these shortcomings by developing separate models, not only for acceleration and deceleration, but also for steady-state responses. Nonlinear regression with robust standard errors was used to estimate the model parameters and obtain the distributions across drivers. The stimulus response thresholds that delimit the acceleration and deceleration responses were determined based on signal detection theory.

Schultz and Rilett [5] proposed a methodology which introduces and calibrates a low parameter distribution using measures of central tendency and dispersion to generate input parameters for car-following sensitivity factors in simulation models using CORSIM. Ten different car-following sensitivity factors were identified to determine the distribution of desired car-following distance and both lognormal and normal distributions were considered under the condition that car-following sensitivity factors fall within range. The results showed that with automated calibration method such as genetic algorithm, the mean absolute error between simulated and observed traffic volume can be minimized.

Using two models of similar complexity (number of parameters): the "Intelligent Driver Model" (IDM) and the "Velocity Difference Model" (VDIFF), Kesting and Treiber [12] researched car-following behaviors on individual drivers using publicly available trajectory data for a straight one-lane road in Stuttgart, Germany. They used a nonlinear optimization procedure based on a genetic algorithm to minimize the deviations between the observed driving dynamics and the simulated trajectory. One of the major findings of the study was that a significant part of the deviations between measured and simulated trajectories can be attributed to the inter-driver variability and the intra-driver variability (stipulating that human drivers do not drive constantly over time, and their behavioral driving parameters change)—the later accounts for a large part of the deviations between simulations and empirical observations.

Menneni et al [13] presented a calibration methodology of the VISSIM Wiedemann car-following model based on integrated use of microscopic and macroscopic data using NGSIM Relative distance vs. relative speed graphs were used for the microscopic calibration, specifically to determine the action points. Scatter and distribution of action points on relative distance versus relative velocity graphs also showed similarity in driver behavior between the two freeways.

Hoogendoorn and Hoogendoorn [14] proposed a generic calibration framework for joint estimation of car following models. The method employed relies on the generic form of most

models and weights each model based on its complexity. This new approach can cross-compare models of varying complexity and even use multiple trajectories when individual trajectory data is scarce. Prior information can also be used to realistically estimate parameter values.

2.3 Methodology

The method employed by this research effort selected, calibrated and compared various car-following models. The models chosen for comparison, shown in Table 2-1, are the following: GHR, Wiedemann, Fritzsche, Gipps, IDM, and VDIFF. These specific models were chosen because they represent a variety of the types of commonly used car following models. Each model was calibrated by the use of a genetic algorithm. A genetic algorithm was used because of its ability to adequately and accurately find the optimal solution when multiple parameters are present like in some of the models.

These models were calibrated using over 100 car following periods for each of the four truck drivers. These four truck drivers were chosen because they represent a wide spectrum of the population. Using the number of driving conflicts each driver experienced in order to classify, Driver B represents a driver with a low number of conflicts, Drivers A and D represent drivers with an average number of conflicts, and Driver C represents a driver with a high number of conflicts. Car-following situations were automatically extracted from the enormous volume of driving data in the database in order to analyze the car following driver behavior. The filtering process is an iterative process where initial values and conditions are used and after the events are flagged they are reviewed in the video data to adjust the values accordingly in order to obtain minimum noise. Visual inspection of the first subsets created revealed some non car-following events so additional filtering was thus performed to remove these events from the database.

Specifically, car following periods were extracted automatically according to these conditions:

- Radar Target ID>0

This eliminates the points in time without a radar target detected

- Radar Range<=120 meters

This represents four seconds of headway at 70 mph

- -1.9 meters<Range*Sin (Azimuth) <1.9 meters

This restricts the data to only one lane in front of the lead vehicle

- Speed>=20km/h

This speed was used in order to minimize the effect of traffic jams, but still leave the influence of congestion in the data

- Rho-inverse <=1/610 meters^{-1}

This limits the curvature of the roadway such that vehicles are not misidentified as being in the same lane as the subject vehicle when roadway curvature is present.

- Length of car following period while the Range is less than 61 meters>= 30 seconds

This criterion was found by trial and error using video analysis to verify positive or negative results.

The automatic extraction process was verified from a sample of events through video analysis. For the random sample of 400 periods, 392 were valid car following periods. The Root Mean Squared Error was calculated based upon the difference in speed between the actual data and the speed given by the different models. This is used for comparison of the models as shown in Table 2-2.

Table 2-1: Table of Car Following models and parameters

GHR	$a_f(t+T_r) = cv_f^m(t+T_r)\frac{\Delta v(t)}{\Delta x^l(t)}$	T_r =time between the observation of a certain stimulus and the reaction on that stimulus $a_f(t+T_r)$ =acceleration of the following vehicle at time $t+T_r$ $v_f(t+T_r)$ = speed of following vehicle at time $t+T_r$ $\Delta v(t)$= relative speed between the following car and the car immediately in front $(v_{leader} - v_{follower})$ $\Delta x(t)$= relative distance between following car and car immediately in front $(x_{leader} - x_{follower})$ m, l, c= parameters describing car following behavior

Gipps	$v_a^n(t+T) =$ $v_c(t) + 2.5\, a_n^{max}\, T\, \left(1 - \frac{v_n(t)}{v_n^{desired}}\right) . \sqrt{0.025 + \frac{v_n(t)}{v_n^{desired}}}$ $v_n^b(t+T) = d_n^{max}.T$ $. \sqrt{(d_n^{max}.T)^2 - d_n^{max}.\left[2\{x_{n-1}(t) - s_{n-1}(t)\} - v_n(t).T - - \frac{v_n(t}{\hat{d}_{n-}}\right.}$	a_n^{max} : Maximum desired acceleration, vehicle n (m/s^2) d_n^{max} : Maximum desired deceleration, vehicle n (m/s^2) $\hat{d}_{n-1}$: Estimation of maximum deceleration desired by vehicle n-1, (m/s^2) s_{n-1} : Effective length of vehicle T: Reaction time $\hat{d}_{n-1}$: Leader desire deceleration x_{n-1} : vehicles spacing
Intelligent Driver Model (IDM)	$a_n(t+\tau) = a\left[1 - \left(\frac{v_n(t)}{v^*}\right)^{\delta} - \left(\frac{\Delta x_{min}^*(v_n(t), \Delta v_{n,n-1(t)})}{\Delta x_{n-1,n}(t)}\right)^2\right]$ $\Delta x_{min}^*\left(v_n(t), \Delta v_{n,n-1(t)}\right) = d + T_{safe} * v_n(t) + \frac{v_n(t)\Delta v_{n,n-1(t)}}{2\sqrt{a^{max} * b^{\max abs}}}$	$\Delta v_{n,n-1}(t)$=approaching rate of the following vehicle v^*=desired speed T_{safe}=safe time headway a^{max}=maximum desired acceleration of following vehicle $b^{\max abs}$=absolute maximum desired deceleration of following vehicle δ acceleration component $\Delta x_{n-1,n}(t)$=distance headway d=vehicle length

Velocity difference model (VDIFF)	$a(s,v,\Delta v)=\frac{v_{opt}(s)-v}{\tau}-\lambda\Delta v$ $v_{opt}(s)=\frac{v_0}{2}\left[tan\left(\frac{s}{l_{int}}-\beta\right)-\tan(-\beta)\right]$	s=distance headway Δv=relative velocity τ=relaxation time λ=sensitivity parameter v_0 =desired velocity l_{int}=interaction length β=form factor
Wiedeman n model	$AX = L_{n-1} + AXadd + RND1_n \times AXmult$ $ABX = AX + BX$ $BX = (BXadd + BXmult \times RND1_n) \times \sqrt{v}$ $v = \begin{cases} v_{n-1}\ for\ v_n > v_{n-1} \\ v_n\ \ for\ v_n \le v_{n-1} \end{cases}$ $SDX = AX + EX \times BX$ $EX = (EXadd + EXmult \times (NRND - RND2_n))$ $SDV = \left(\frac{\Delta x - L_{n-1} - AX}{CX}\right)^2$ $CX = CXconst \times (CXadd + CXmult \times (NRND1_n + RND2_n))$ $OPDV = CLDV \times (-OPDVadd - OPDVmult \times NRND)$ $AD = S_{n-1} + T_D \times v_n$ $AR = S_{n-1} + T_r \times v_{n-1}$ $AS = S_{n-1} + T_s \times v_n$ $\Delta b_m = \lvert b_{min}\rvert + a_{n-1}$ $AB = AR + \frac{\Delta v^2}{\Delta b_m}$	AX: the desired distance between stationery vehicles ABX: the desired minimum following distance at low speed differences SDX: the threshold for maximum following distance SDV: the point which the driver notice that he approach a slower vehicle. OPDV : Increasing speed difference, L_{n-1} : The leading vehicle length *AXadd* and *AXmult* are calibration parameters $RND1_n$ is a normal distributed random number for vehicle (n) v: Vehicle speed *CXconst*, *CXadd* and *CXmult*i are calibration

		parameters *NRDV* is a normally distributed random number *OPDVadd* and *OPDVmult* are calibration parameters
Fritzsche	$AD = S_{n-1} + T_D \times v_n$ $AR = S_{n-1} + T_r \times v_{n-1}$ $AS = S_{n-1} + T_s \times v_n$ $\Delta b_m = \lvert b_{min} \rvert + a_{n-1}$ $AB = AR + \frac{\Delta v^2}{\Delta b_m}$	AD: desired distance threshold AR: risk distance threshold AS: The safe distance threshold AB: The risk braking distance threshold T_D : Parameter represents the desire time gap S_{n-1}: Effective length of vehicle v_n : following vehicle speed T_r : Parameter represents the risky time gap T_s : Parameter represents the safe distance gap b_{min} , a_{n-1} : Parameter controlling maximum deceleration

Table 2-2: Root Mean Squared Error for each model by Driver

	Driver A	Driver B	Driver C	Driver D
GHR	0.9294	0.9533	1.1892	4.3815
Gipps	1.3894	1.2036	2.3112	3.8024
IDM	1.2260	1.2215	1.9211	1.0985
Vdiff	1.1082	1.0848	1.1990	1.2454
Wiedemann	0.7541	1.0916	1.4735	1.0764
Fritzsche	2.2094	1.3413	1.4332	1.1242

Table 2-3 shows the Sum of Squared Error for each model by Driver. The right most column presents the Root Mean Squared Error if the Sum of Squared Error is summed for all the drivers and then converted to a Root Mean Squared Error. This provides a means of comparison of the different models, if a single model were to be used for all of the drivers. The results show that the Wiedemann model results in the least Root Mean Squared Error with the Velocity Difference model (VDIFF) not being far behind.

Table 2-3: Sum of Squared Error for the models by driver with a Root Mean Squared Error of the Total

	Driver A	Driver B	Driver C	Driver D	Total	RMSE
GHR	78774	104980	177220	1752741	2113714	2.2345
Gipps	176030	167333	669436	1320099	2332898	2.3475
IDM	137063	172342	462506	110167	882078	1.4435
Vdiff	111990	135938	180169	141616	569713	1.1601
Wiedemann	51749	108426	197567	105430	463172	1.0460
Fritzsche	445138	207813	257427	115386	1025765	1.5566

Table 2-4 shows the parameter values of the GHR model for each driver. The GHR model showed the least Root Mean Squared Error for two of the drivers, but with the inclusion of the other drivers, this model shows a higher Root Mean Squared Error than some of the other models. This fact only means that the GHR model can accurately mimic some drivers, but it is not sufficient to model all the drivers presented here. The structure of the model causes this to occur because some of the drivers exhibit behavior that is more complex than the GHR model can handle.

Table 2-4: GHR Parameter Values by Driver

	Driver A	Driver B	Driver C	Driver D
c	-3.553	-0.959	-0.542	0.300
m	-0.253	0.264	1.068	0.000
l	0.644	0.576	1.000	1.000
T	1.791	0.272	1.087	1.000
RMSE	0.929	0.953	1.189	4.381

Table 2-5 presents the calibrated parameters of the Gipps model for each of the drivers. The Gipps model does not calibrate as well as the other models as shown by the Root Mean Squared Error. The Gipps model shows a large increase in error in Drivers C and D as compared to Drivers A and B. Table 2-3 suggests that the Gipps model is not as adequate as the other model when representing multiple drivers. The Gipps model is originally a two-regime macroscopic traffic flow model and that characteristic is obvious when it is compared to other microscopic models as this model tends to represent "steady state" behavior.

Table 2-5: Gipps Parameter Values by Driver

	Driver A	Driver B	Driver C	Driver D
b	0.2105	0.2740	-0.0164	-0.4231
b'	6.3986	9.7948	0.5938	0.0916
Ln-1	90.1440	19.3718	10.5249	3.0981
Un	92.1683	135.6518	26.4435	25.0118
an	7.3557	7.9477	-0.0004	0.5487
T	1.9306	0.9083	0.9974	0.2282
RMSE	1.3894	1.2036	2.3112	3.8024

Table 2-6 presents the calibrated parameters of the Intelligent Driver model for the four drivers. The Intelligent Driver Model shows a Root Mean Squared Error very similar to the Wiedemann model for Driver D, but higher Root Mean Squared Error values for the other drivers. In Table 2-3, the Intelligent Driver model shows a Root Mean Squared Error that suggests that it is better at representing multiple drivers than a couple other models, but it is not as adequate as other models. This means that the Intelligent Driver Model is not as accurate as other models when

representing one driver, but when multiple drivers are considered, it can outperform a couple of the other models.

Table 2-6: IDM Parameter Values by Driver

	Driver A	Driver B	Driver C	Driver D
a	2.6519	3.3372	5.8950	0.8724
vdes	106.5559	97.3445	144.7275	96.0030
s0	27.5776	8.8639	2.5513	15.6821
T	0.0831	2.2913	2.3686	2.1768
b	1.0143	1.0593	67.6662	0.3113
RMSE	1.2260	1.2215	1.9211	1.0985

Table 2-7 presents the calibrated parameters for the Velocity Difference model of the four drivers. The values of the free flow speed and desired velocity suggest that their use in this model will only cause error and that a replacement with a calibration parameter would yield a more accurate representation of the actual behavior of drivers. The Velocity Difference model shows a Root Mean Squared Error that is similar and not too distant from the Wiedemann model. The Velocity Difference model also shows very stable behavior across the different drivers in Table 2-2. This shows that the Velocity Difference model can adequately represent the behavior of different drivers in a manner that exceeds or is on par with the other models.

Table 2-7: VDIFF Parameter Values by Driver

	Driver A	Driver B	Driver C	Driver D
FFS	48.5177	79.9246	123.4765	155.2547
Ln	5.0480	50.4894	36.6056	17.3944
Lag time	0.9870	3.5970	0.2989	2.4494
Sensitivity	12.7509	13.6386	1.0580	8.2774
Vdes	93.1806	106.0174	33.6502	76.6298
Form factor	4.6059	6.9404	0.9134	7.1708
l	8.2814	6.0162	6.6070	5.2652
tau	4.4006	3.4847	1.3662	2.9527
RMSE	1.1082	1.0848	1.1990	1.2454

Table 2-8 shows the calibrated parameters of the Wiedemann model for the four drivers. The drivers show different null acceleration values and different threshold parameters which highlights that the drivers have different preferences for accelerating and decelerating while following. This also shows that the drivers make the decision to change accelerations at different points. The flexibility available in the Wiedemann undoubtedly contributes to its performance in mimicking the behavior of real drivers. The Wiedemann model shows stable behavior across the different drivers like the Velocity Difference model, but with a small hiccup in Driver C. The Intelligent Driver model and the Gipps model showed this same hiccup in Driver C. Nevertheless, the Wiedemann model shows a good performance for representing different drivers as shown in Table 2-3.

Table 2-8: Wiedemann Parameter Values by Driver

	Driver A	Driver B	Driver C	Driver D
Ln-1	4.4938	5.5533	4.5469	5.6797
AX	2.5254	5.0441	2.8730	5.6009
BX	3.0408	3.4054	3.4211	3.4349
EX	2.5139	3.0961	3.4273	2.6760
CX	40.0659	75.0421	62.4053	93.1305
CX2	39.0314	28.9785	73.2578	73.0260
CLDVCX	31.7622	56.7976	33.1589	51.0795
OPDV	-2.5116	-6.5796	-1.0677	-3.3071
bnull	0.1224	0.0747	0.2408	0.0716
bmaxmult	0.0991	0.1533	0.4271	0.3871
FaktorVmult	0.0389	0.1670	0.2002	0.1820
bminadd	-20.8984	-13.1674	-23.4076	-41.7209
bminmult	0.0334	0.0913	0.3202	0.3784
Vdes	42.6738	84.0379	88.7207	16.0671
FaktorV	0.9396	0.5216	0.5065	1.9585
RMSE	0.7541	1.0916	1.4735	1.0764

Table 2-9 presents the calibrated parameters of the Fritzsche model for the four drivers. The model shows similar null acceleration values for three of the drivers. Three of the drivers also show similar an-1 and an+ values. The Fritzsche model is very similar to the Wiedemann model in the way it operates, but the Root Mean Squared Error shows that the Fritzsche model does not perform similar to the Wiedemann model. The Fritzsche model shows a competitive Root Mean Squared Error for Driver D, but lacks with the other drivers. This inconsistency shows in Table

2-3 with the Fritzsche model having mediocre performance compared to the other models which highlights its inadequacy to mimic multiple drivers.

Table 2-9: Fritzsche Parameter Value by Driver

	Driver A	Driver B	Driver C	Driver D
Sn-1	22.6295	2.0673	2.0673	1.8332
kPTN	5.4213	4.8326	4.8326	4.0063
kPTP	1.1493	3.0874	3.0874	1.9313
fx	19.3430	-62.8779	-62.8779	-62.5547
Td	4.4129	4.8104	4.8104	3.9579
Tr	1.8111	0.8955	0.8955	1.0082
Ts	2.9147	3.6792	3.6792	3.8147
bmin	-2.4743	-0.0955	-0.0955	-0.8210
an-1	-4.5296	6.8066	6.8066	6.0010
bnull	-6.0129	6.7731	6.7731	6.4286
an+	-5.3233	-5.3827	-5.3827	-3.5638
RMSE	2.2094	1.3413	1.4332	1.1242

Figure 2-1 presents an example fitted car following period for Driver D that is representative of the observations seen in other car following periods for all four drivers. Most of the models show a behavior that is heavily influenced by the lead vehicle as shown by the lines for the models overlapping the line for the lead vehicle in Figure 2-1. The actual behavior of the driver shows less dependence upon the behavior of the lead vehicle as shown by the black line in Figure 2-1. The GHR and Gipps models show large error in this car following period. The error of the Gipps model is the constant velocity, while the error of the GHR model appears to be that this car following period represents behavior that the calibrated GHR model does not adequately capture. The rest of the models show similar behavior that, as mentioned before, is heavily influenced by the actions of the lead vehicle.

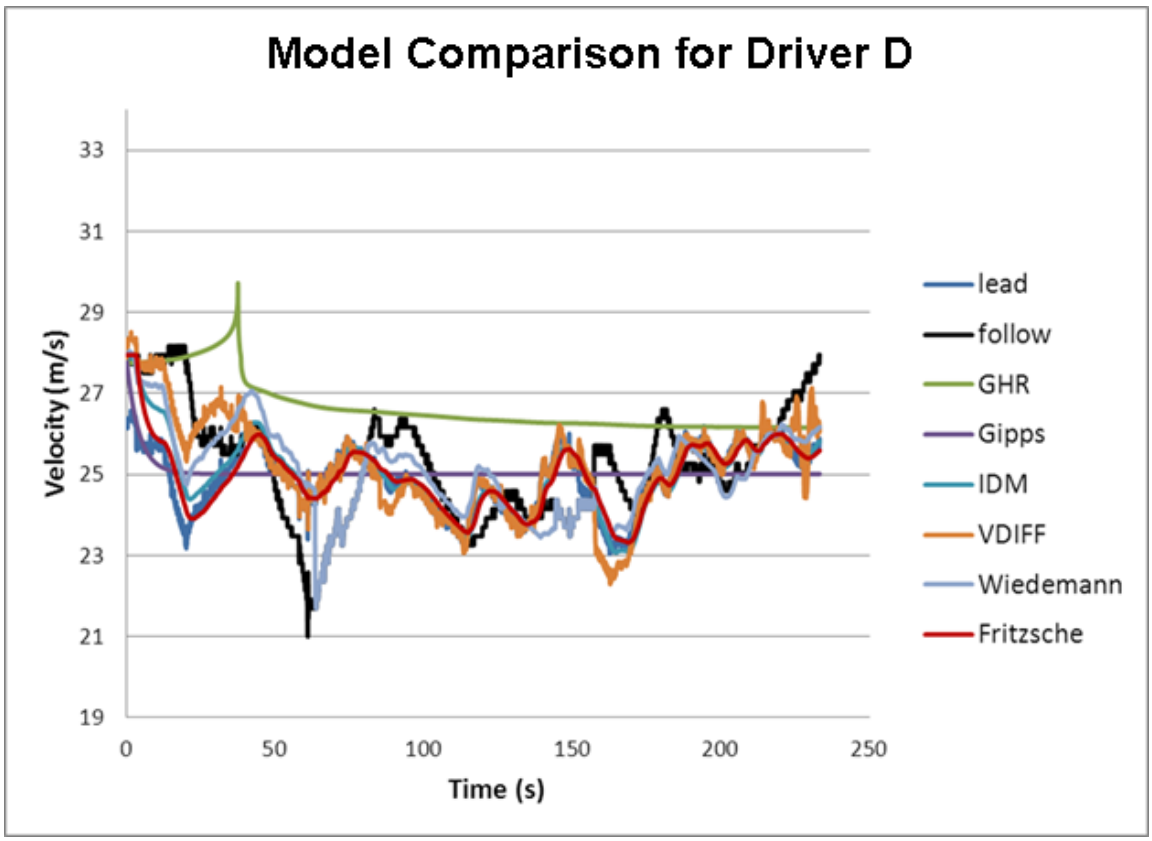

Figure 2-1: Plot of models as compared to the data for Driver D.

2.4 Conclusions

The results show that some of the microscopic traffic flow models calibrate to match the actual driver better than others. The results also show that some of the models are more adequate at mimicking different truck drivers. Most of the models show a behavior that is heavily influenced by the actions of the lead vehicle. The results of this research effort support that the Velocity Difference model and the Wiedemann model can adequately represent the behavior of different drivers. This means that if a single car following model is used with data from different drivers individually, these two models show the most promise in being up to the task. It is important to note that these findings are based solely upon data for truck drivers, so the applicability of these findings to car driver behavior would be questionable and thus would be recommended as an area of future research. Further research is also recommended in testing these two models with a larger number of individual drivers in order to clarify the strengths and weaknesses of each model.

Acknowledgment

This material is based upon work supported by the Federal Highway Administration under Agreement No. DTFH61-09-H-00007. Any opinions, findings, and conclusions or recommendations expressed in this publication are those of the Author(s) and do not necessarily reflect the view of the Federal Highway Administration.

The authors would like to express thanks to Dr. C.Y. David Yang, the FHWA Agreement Manager, for his continued support and guidance during this project. They would also like to thank individuals at Virginia Tech and the Virginia Tech Transportation Institute who contributed to the study in various ways: Greg Fitch, Shane McLaughlin, Kelly Stanley and Rebecca Olson.

References

1. Olson, R., et al., *DRIVER DISTRACTION IN COMMERCIAL VEHICLE OPERATIONS*. 2009, Center for Truck and Bus Safety Virginia Tech Transportation Institute: Blacksburg VA. p. 285.
2. Ranjitkar, P. and T. Nakatsuji, *A TRAJECTORY BASED ANALYSIS OF DRIVERS' RESPONSE IN CAR FOLLOWING SITUATIONS.* TRB 2010 Annual Meeting CD-ROM, 2010: p. 21.
3. Ossen, S. and S.P. Hoogendoorn, *Validity of trajectory-based calibration approach of car-following models in presence of measurement errors.* Transportation Research Record, 2008(2088): p. 117-125.
4. Brackstone, M., *Driver Psychological Types and Car Following:Is There a Correlation? Results of a Pilot Study*. 2003. p. 6.
5. Schultz, G.G. and L.R. Rilett, *Analysis of Distribution and Calibration of Car-Following Sensitivity Parameters in Microscopic Traffic Simulation Models.* 2004: p. 11.
6. Panwai, S. and H. Dia, *Comparative evaluation of microscopic car-following behavior*. IEEE TRANSACTIONS ON INTELLIGENT TRANSPORTATION SYSTEMS, 2005. **6**(3): p. 314-325.
7. Siuhi, S. and M. Kaseko, *PARAMETRIC STUDY OF STIMULUS-RESPONSE BEHAVIOR FOR CAR-FOLLOWING MODELS.* TRB 2010 Annual Meeting CD-ROM, 2010.
8. Osaki, H., *Reaction and anticipation in the Car-Following Behavior*. In Proceedings of the 12 International Symposium on the Theory of Traffic Flow and Transportation, 1993.
9. Subranmanian, H., *Estimation of Car-Following Models.* Master Thesis, 1996.
10. Ahmed, K.I., *Modeling Drivers' Acceleration and Lane Changing Behavior.* PhD Dissertation, 1999.
11. Toledo, T., *Integrating Driving Behavior.* PhD Dissertation,, 2003.
12. Kesting, A. and M. Treiber, *Calibrating Car-Following Models using Trajectory Data: Methodological Study.* 2008: p. 17.
13. Menneni, S., C.P.D. Sun, P.E., and P. Vortisch, *An Integrated Microscopic and Macroscopic Calibration for Psycho-Physical Car Following Models* TRB 2009 Annual Meeting CD-ROM 2008: p. 17.
14. Hoogendoorn, S. and R. Hoogendoorn, *A Generic Calibration Framework for Joint Estimation of Car Following Models using Microscopic Data.* TRB 2010 Annual Meeting CD-ROM, 2010: p. 17.

3. ANALYSIS OF THE WIEDEMANN CAR FOLLOWING MODEL OVER DIFFERENT SPEEDS USING NATURALISTIC DATA[2]

Abstract

This research effort analyzes the Wiedemann car-following model using car-following periods that occur at different speeds. The Wiedemann car-following model uses thresholds to define the different regimes in car following. Some of these thresholds use a speed parameter, but others rely solely upon the difference in speed between the subject vehicle and the lead vehicle. The results show that the thresholds are not constant, but vary over different speeds. Another interesting note is that the variance over the speeds appears to be driver dependent. The results indicate that the drivers exhibit different behaviors depending upon the speed which can imply an increase in aggression at particular speeds.

[2] Paper accepted for presentation at the 3rd International Conference on Road Safety and Simulation

3.1 Background

The Wiedemann car-following model was originally formulated in 1974 by Rainer Wiedemann [1] . This model is known for its extensive use in the microscopic multi-modal traffic flow simulation software, VISSIM [2]. The Wiedemann model was constructed based on conceptual development and limited available data, and has to be calibrated to specific traffic stream data.

The principal ideas behind the Wiedemann model were used in this paper, but the exact shape or formula used in the model are updated using the Naturalistic Driving data that is deemed to be one of the best available sources of "real world" data [3].

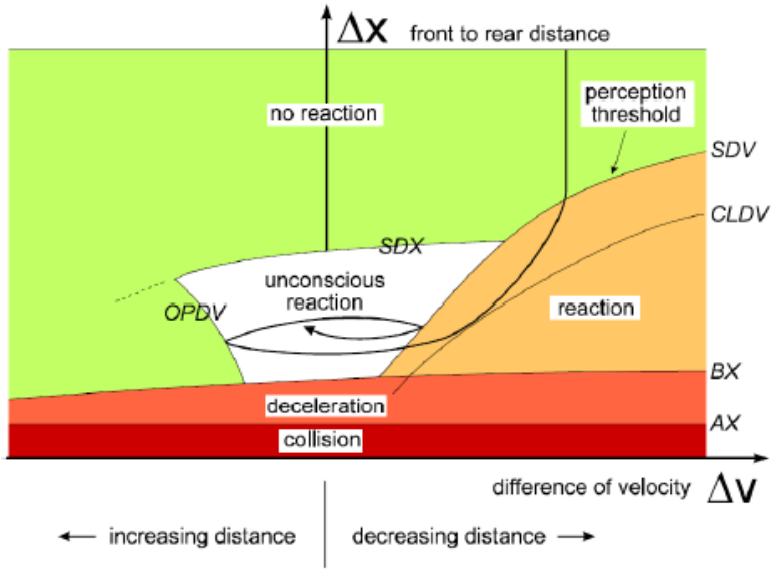

Figure 3-1: Wiedemann 74 Car Following Logic [2]

Figure 3-1 shows the graphical form of the Wiedemann 74 model. The different thresholds are shown with a certain shape that can only be amplified during the calibration procedure. The figure shows the subject vehicle approaching a lead vehicle (ΔX decreasing due to higher subject vehicle's speed shown by a positive ΔV), and entering a perception area (crossing the SDV threshold) where it has to reduce speed. The subject vehicle then crosses another threshold (CLDV) where it reacts and reduces speed even further to enter an unconscious reaction car-following episode. The subject vehicle then continues the unconscious car-following episode as long as it remains bounded by the OPDV, SDX, and SDV thresholds.

3.2 Advantages of naturalistic data

As opposed to traditional epidemiological and experimental / empirical approaches, this *in situ* process uses drivers who operate vehicles that have been equipped with specialized sensors along with processing and recording equipment. In effect, the vehicle becomes the data collection device. The drivers operate and interact with these vehicles during their normal driving routines while the data collection equipment is continuously recording numerous items of interest during the entire driving. Naturalistic data collection methods require a sophisticated network of sensor, processing, and recording systems.

This system provides a diverse collection of both on-road driving and driver (participant, non-driving) data, including measures such as driver input and performance (e.g., lane position, headway, etc.), four camera video views, and driver activity data. This information may be supplemented by subjective data, such as questionnaire data.

As part of the Naturalistic Truck Driving Study DS study [3], one hundred drivers were recruited from four different trucking fleets across seven terminals and one to three trucks at each trucking fleet were instrumented (nine trucks total). After a participant finished 4 consecutive weeks of data collection, another participant started driving the instrumented truck. Three forms of data were collected by the NTDS DAS: video, dynamic performance, and audio. Approximately 14,500 driving-data hours covering 735,000 miles traveled were collected. Nine trucks were instrumented with the DAS.

The following is a typical description of how the data collection is performed, along with accompanying screen shots and information describing how the system works and how data can be used. Four cameras monitor and record the driver's face, forward road view, and left- and right-side of the tractor trailer, which are used to observe the traffic actions of other vehicles around the vehicle. Low-level infrared lighting (not visible to the driver) illuminates the vehicle cab so the driver's face and hands could be viewed via the camera during nighttime driving. The sensor data associated with the project were originally collected in a proprietary binary file format. A database schema was devised and the necessary tables were created. The schema preserves the organization of data into modules; i.e., all of the variables associated with a particular module are stored in one table in the database. The import process itself consisted of reading the binary files, writing the data to intermediate comma separated value (CSV) files and "bulk inserting" the CSV files into the database. A stored procedure is available that allows one to query the database using the module and variable names rather than database table and column names.

3.3 Synthesis of past efforts

There have been many attempts to characterize the car-following behavior of drivers. However, direct correlation with real driving variables is rare and parameterization of objective behavior is still in its development. Some studies have been limited to very controlled experiments; recent studies have used aerial photography based measurement from helicopters [4], GPS data, test track data and trajectory data form NGSIM .

Ossen and Hoogendoorn [5] studied the car-following behavior of individual drivers using vehicle trajectory data that were extracted from high-resolution digital images collected at a high frequency from a helicopter. The analysis was performed by estimating the parameters of different specifications of the GHR car-following rule for individual drivers. In 80 % of the cases, a statistical relation between stimuli and response could be established. The Gipps (a safe distance model) and Tampere (stimulus-response model) models and a synthetic data based approach were used for assessing the impact of measurement errors on calibration results. According to the authors, the main contribution of their study was that considerable differences between the car-following behaviors of individual drivers were identified that can be expressed in terms of different optimal parameters and also as different car-following models that appear to be optimal based on the individual driver data. This is an important result taking into account that in

most models a single car-following rule is used. The authors also proposed for future research to apply more advanced statistical methods and to use larger databases.

Brackstone [6] using data collected with an instrumented vehicle that was assembled at TRG Southampton parameterize the Wiedemann's threshold for a typical following spiral. As a result they represent the action points as a function of a probability distribution based on ground speed.

Micro-simulation software packages use a variety of car-following models including Gipps' (AIMSUN, SISTM, and DRACULA), Wiedemann's (VISSIM), Pipe's (CORSIM), and Fritzsche's (PARAMICS). And different automated calibration parameters such as genetic algorithms have been used to calibrate the distribution of car-following sensitivity parameters *[7]*. Panwai and Dia [8] compared the car-following models between different simulation software, including AIMSUN, PARAMICS and VISSIM using an instrumented vehicle to record differences in speed and headway (Leading speed, relative distance, relative speed, follower acceleration were recorded). The EM shows similar values for psychophysical models in VISSIM and PARAMICS and lower values in AIMSUN. The RMS error and qualitative drift and goal-seeking analyses also showed a substantially different car-following behavior for PARAMICS.

Siuhi and Kaseko [9] demonstrated the need for separate models for acceleration and deceleration responses by developing a family of car-following models and addressing the shortcomings of the GM model. Previous work from Osaki [10] and Subranmanian [11] modified the GM model separating the acceleration and deceleration responses. Ahmed [12], following some work from Subranmanian assumed non linearity in the stimulus term and introduced traffic density. Results from Ahmed [12] and Toledo [13] showed , against popular belief, that acceleration increases with speed but decreases with vehicle separation. Due to statistical insignificance, Ahmed and Toledo also removed speed from their deceleration models. Siuhi and Kasvo [9] addressed some of these shortcomings by developing separate models, not only for acceleration and deceleration, but also for steady-state responses. Nonlinear regression with robust standard errors was used to estimate the model parameters and obtain the distributions across drivers. The stimulus response thresholds that delimit the acceleration and deceleration responses were determined based on signal detection theory.

Menneni et al [14] presented a calibration methodology of the VISSIM Wiedemann car-following model based on integrated use of microscopic and macroscopic data using NGSIM Relative distance vs. relative speed graphs were used for the microscopic calibration, specifically to determine the action points (it is important to note that action points were not identical to perception threshold). Scatter and distribution of action points on relative distance versus relative velocity graphs also showed similarity in driver behavior between the two freeways. Menneni also mentioned that many of the Wiedemann thresholds are velocity dependent, but a full calibration with this third dimension would be a daunting task.

Hoogendoorn and Hoogendoorn [15] proposed a generic calibration framework for joint estimation of car following models. The method employed relies on the generic form of most models and weights each model based on its complexity. This new approach can

cross-compare models of varying complexity and even use multiple trajectories when individual trajectory data is scarce. Prior information can also be used to realistically estimate parameter values.

3.4 Description of the Wiedemann Model

The Wiedemann model uses random numbers in order to create heterogeneous traffic stream behavior in VISSIM. These random numbers are meant to simulate behavior of different drivers. The naturalistic data is a perfect match for this situation because the data is collected by individual drivers. Data for three different drivers was selected and processed in order to calibrate the Wiedemann car-following model. Specifically, car following periods were extracted automatically according to these conditions for each speed range:

- Radar Target ID>0

This eliminates the points in time without a radar target detected

- Radar Range<=120 meters

This represents four seconds of headway at 70 mph

- -1.9 meters<Range*Sin (Azimuth) <1.9 meters

This restricts the data to only one lane in front of the lead vehicle

- 20>=Speed>=110

This criterion would be further defined by the different speed ranges.

- Rho-inverse <=1/610 meters^{-1}

This limits the curvature of the roadway such that vehicles are not misidentified as being in the same lane as the subject vehicle when roadway curvature is present.

- Length of car following period while range is less than 61 meters >= 30 seconds

This criterion was established by trial and error as verified by video analysis.

The automatic extraction process was verified from a sample of events through video analysis. For the random sample of 400 periods, 392 were valid car following periods.

The data was divided into the following speed ranges: 20-30 kph, 30-40 kph, 40-50 kph, 50-60 kph, 60-70 kph, 70-80 kph, 80-90 kph, 90-100 kph, and 100-110 kph.

The equations that form the Wiedemann model were altered in order to remove the random parameters because they were not necessary when calibrating to a single driver. The equations shown are the altered equations which reduces the number of calibration parameters. The starting point for the Wiedemann model is the desired distance between stationary vehicles. The value calculated by Equation 3-1 is used in the calculations for the other thresholds.

$$\boldsymbol{AX = L_{n-1} + AXadd} \qquad (3\text{-}1)$$

L_{n-1} is the length of the lead vehicle

$AXadd$ is a calibrated parameter

The desired minimum following distance threshold is calculated using Equation 3-2 and Equation 3-3.

$$\boldsymbol{ABX = AX + BX} \qquad (3\text{-}2)$$

$$\boldsymbol{BX = BXmult * \sqrt{v}} \qquad (3\text{-}3)$$

$BXmult$ is a calibration parameter

v is the minimum of the speed of the subject vehicle and the lead vehicle

The maximum following distance is calculated using Equation 3-4 and Equation 3-5.

$$\boldsymbol{SDX = AX + EX * BX} \qquad (3\text{-}4)$$

$$\boldsymbol{EX = EXmult} \qquad (3\text{-}5)$$

$EXmult$ is a calibration parameter.

The Perception Threshold marks the point that a driver will begin to react to the lead vehicle. This threshold is calculated by the use of Equation 3-6. Equation 3-1 is needed in order to calculate Equation 3-6.

$$\boldsymbol{SDV = \left(\frac{\Delta x - L_{n-1} - AX}{CX}\right)^2} \qquad (3\text{-}6)$$

L_{n-1} is the length of the lead vehicle.

CX is a calibrated parameter

The reaction curve marks the location of a second acceleration change point while still closing on the lead vehicle. In VISSIM this threshold is assumed to be equivalent to the Perception Threshold. Due to that similarity, the equation used for the Reaction Threshold, Equation 3-7 is derived from Equation 3-6.

$$\boldsymbol{CLDV = \left(\frac{\Delta x - L_{n-1} - AX}{CLDVCX}\right)^2} \qquad (3\text{-}7)$$

$CLDVCX$ is a calibrated parameter specific to one driver

The OPDV (Opening Difference in Velocity) curve is primarily a boundary to the unconscious reaction region. It represents the point where the driver notices that the distance between his or her vehicle and the lead vehicle is increasing over time. When this realization is made the driver will accelerate in order to maintain desired space headway. This threshold is calculated using Equation 3-8.

$$\boldsymbol{OPDV = CLDV * OPDVmult} \quad (3\text{-}8)$$

$OPDVmult$ is a calibrated parameter

The Wiedemann model reuses the Perception Threshold as a boundary to the unconscious reaction region. This would again be the point where the driver notices that the distance between his or her vehicle and the lead vehicle is decreasing over time, but this second use of the threshold is used when the subject vehicle is already engaged in following the lead vehicle. In our representation of the model, this reuse of the Perception Threshold was given its own equation in order to separate the different uses of the threshold. Equation 3-9 is of the same form as Equation 3-6, but with a different calibrated parameter.

$$\boldsymbol{SDV2 = \left(\frac{\Delta x - L_{n-1} - AX}{CX2}\right)^2} \quad (3\text{-}9)$$

$CX2$ is a calibrated parameter

The first state is the free driving regime where the subject vehicle is not reacting to a lead vehicle and is travelling at a desired speed or accelerating to a desired speed. The Free Driving Regime is defined as the area above the Perception Threshold and the Maximum Following Distance Threshold. If the subject vehicle enters the free driving regime, the subject vehicle will then accelerate until the desired speed is reached. The value for this acceleration is calculated using Equation 3-10 and Equation 3-11. Equation 3-10 relates the maximum speed to the current speed times Equation 3-11 and calculates an acceleration value accordingly in order to reach the maximum speed.

$$\boldsymbol{b_{max} = BMAXmult * (v_{max} - v * FaktorV)} \quad (3\text{-}10)$$

$BMAXmult$is a calibration parameter

$v_{max}$is the maximum speed of the vehicle

$$\boldsymbol{FaktorV = FAKTORVmult} \quad (3\text{-}11)$$

$FAKTORVmult$ is a calibration parameter

The approaching regime occurs when a vehicle in the Free Driving Regime passes the Perception Threshold. This vehicle will then decelerate according to Equation 3-12.

$$\boldsymbol{b_n = \frac{1}{2}\frac{(\Delta v)^2}{ABX - (\Delta x - L_{n-1})} + b_{n-1}} \quad (3\text{-}12)$$

The Closely Approaching regime occurs only when a vehicle in the approaching regime passes the Closing Difference in Velocity Threshold. In VISSIM this regime is ignored, so the deceleration is still calculated by Equation 3-12.

The Deceleration Following regime occurs as a result of a vehicle in the Approaching or Closely Approaching regime passes the Perception Threshold or a vehicle in the Acceleration Following Regime passes the Second Perception Threshold. When a

vehicle enters the Deceleration Following regime the acceleration is calculated by the negative of Equation 3-13.

$$\boldsymbol{b_{null}} = \boldsymbol{b_{null}} \quad (3\text{-}13)$$

$\boldsymbol{b_{null}}$ is a calibrated parameter

The Acceleration following regime occurs when a vehicle in the Deceleration Following regime passes the Opening Difference in Velocity Threshold or a vehicle in the Emergency Regime passes the Minimum Following Distance Threshold. The acceleration for a vehicle in the Acceleration following regime is simply the positive value of Equation 3-13. If a vehicle in this regime accelerates and crosses the Maximum Following Distance Threshold, then that vehicle will enter the Free Driving regime. Also, the vice-versa is true where a vehicle will enter the Acceleration following regime from the Free Driving Regime if the Maximum Following Distance Threshold is passed.

The emergency regime occurs any time that the space headway is below the Minimum Following Distance Threshold. Equation 3-14 and Equation 3-15 calculate the acceleration in the Emergency regime.

$$\boldsymbol{b_n} = \frac{\mathbf{1}}{\mathbf{2}} \frac{(\Delta \boldsymbol{v})^{\mathbf{2}}}{\boldsymbol{ABX} - (\Delta \boldsymbol{x} - \boldsymbol{L_{n-1}})} + \boldsymbol{b_{n-1}} + \boldsymbol{b_{min}} * \frac{\boldsymbol{ABX} - (\Delta \boldsymbol{x} - \boldsymbol{L_{n-1}})}{\boldsymbol{BX}} \quad (3\text{-}14)$$

$$\boldsymbol{b_{min}} = \boldsymbol{BMINadd} + \boldsymbol{BMINmult} * \boldsymbol{v_n} \quad (3\text{-}15)$$

$BMINadd, BMINmult$ are calibration parameters

v_n is the speed of the subject vehicle

The adjusted equations were implemented into a calibration framework that used a genetic algorithm to calculate the optimal values of the parameters. A genetic algorithm was used because of its ability to accurately find optimal solutions that meet certain criteria when numerous parameters are present. The framework consisted of expressing the logic of the Wiedemann model as a series of state transitions. The states are defined by the different thresholds and each state has an equation or parameter for the acceleration. The optimization function was simply the minimization of the error between the velocity values calculated in the Wiedemann model and the velocity values directly from the data.

3.5 Evaluation of the Wiedemann Model over Different Speed Ranges

Results of the calibration for a sample driver (Driver B) over a different speed ranges is shown in Table 3-1. The length of the lead vehicle (Ln-1) shows feasible results across all of the ranges, which serves to validate the results of the calibration. The desired speed (Vdes) shows erratic behavior in the results. Vdes, FaktorVmult, and bmaxmult are all used to calculate the acceleration in the free driving regime. Judging from the variance in these parameters, the acceleration equation for the free driving regime needs to be re-evaluated.

The parameters BX and EX show smaller variance than CX, CX2, CLDVCX, and OPDV over the different speed ranges. This can be attributed to the equations that use these

parameters. The equations with BX and EX include a velocity term while the other parameters have to account for the differences that speed causes. The null acceleration or bnull shows an interesting trend of high accelerations at low velocities and low acceleration at high velocities.

Table 3-1: Driver B Wiedemann Parameter Results

	20-30 kph	30-40 kph	40-50 kph	50-60 kph	60-70 kph	70-80 kph	80-90 kph	90-100 kph	100-110 kph
Ln-1	5.586	5.623	5.461	5.795	4.805	5.084	4.419	4.322	5.906
AXadd	4.540	6.941	9.611	9.152	5.613	6.230	7.899	9.187	9.890
BX	3.781	4.016	3.647	4.260	4.506	3.733	3.578	3.563	4.318
EX	2.974	3.659	3.257	3.582	3.491	2.774	2.855	3.115	3.842
CX	19.511	26.612	19.798	92.114	83.621	90.067	78.938	55.382	17.806
CX2	95.072	75.897	19.459	77.140	74.041	51.673	37.506	53.216	68.893
CLDVCX	15.518	24.870	18.487	57.298	57.721	57.315	76.277	48.422	10.000
OPDV	-3.947	-2.739	-2.299	-2.533	-2.241	-1.827	-7.024	-2.665	-5.872
bnull	0.194	0.228	0.140	0.158	0.174	0.110	0.121	0.063	0.000
bmaxmult	0.004	0.105	0.318	0.223	0.137	0.127	0.391	0.367	0.294
FaktorVmult	0.328	0.146	0.189	0.242	0.446	0.267	0.217	0.067	0.152
bminadd	-1.696	-46.706	-48.703	-47.311	-2.376	-23.471	-39.434	-18.901	-26.656
bminmult	0.283	0.332	0.124	0.081	0.085	0.336	0.319	0.170	0.247
Vdes	100.492	86.696	16.415	51.215	52.278	90.280	120.000	39.789	34.743
FaktorV	0.496	0.501	1.916	0.825	0.855	0.521	0.390	1.005	1.125
RMSE	0.905	1.067	0.863	0.821	1.177	0.639	0.807	0.719	0.576

Table 3-2 presents the calibration results for another driver (Driver C) over varying speed ranges. The length of the lead vehicle (Ln-1) shows feasible values across the speed ranges which validates the calibration results. Like Driver B's results, the BX and EX terms shows smaller variance than the other parameters. The null acceleration (bnull) reveals some interesting behavior in Driver C that is different from Driver B. Remembering that bnull represents the acceleration and deceleration behavior of drivers while oscillating, the null acceleration can be used to identify when a driver has more relaxed or more aggressive acceleration and deceleration behavior while following. The

higher bnull values correspond to the lower SDV2 thresholds in **Error! Reference source not found.** with the exception on the 20-30 kph range. This means that Driver C has a larger following regime, graphically speaking, where the larger acceleration values exist. This correlation combines to create larger oscillation loops in the following behavior which can indicate a less attentive state than smaller oscillation loops.

Table 3-2: Driver C Wiedemann Parameter Results

	20-30 kph	30-40 kph	40-50 kph	50-60 kph	60-70 kph	70-80 kph	80-90 kph	90-100 kph	100-110 kph
Ln-1	4.123	6.000	4.305	4.151	4.172	5.407	4.133	4.322	5.016
AXadd	7.958	10.000	4.788	1.108	8.759	9.772	4.576	9.187	5.917
BX	4.678	4.250	4.406	3.175	3.770	4.666	3.152	3.563	4.224
EX	3.157	2.517	2.922	2.615	2.570	3.260	3.887	3.115	3.326
CX	94.615	71.029	48.788	19.926	32.200	88.899	90.181	55.382	65.713
CX2	70.870	81.272	43.778	100.000	45.590	36.588	70.846	53.216	54.886
CLDVCX	42.323	51.518	43.741	11.094	31.156	60.460	66.929	48.422	39.959
OPDV	-5.206	-3.484	-4.585	-3.510	-2.269	-3.395	-4.081	-2.665	-3.380
bnull	1.000	0.085	0.287	0.221	0.451	0.912	0.061	0.063	0.000
bmaxmult	0.356	0.285	0.075	0.089	0.113	0.400	0.249	0.367	0.190
FaktorVmult	0.085	0.255	0.450	0.218	0.304	0.409	0.288	0.067	0.155
bminadd	-29.008	-22.619	-9.219	-17.026	-23.879	-23.877	-11.057	-18.901	-31.202
bminmult	0.232	0.335	0.400	0.024	0.085	0.277	0.084	0.170	0.253
Vdes	18.872	35.610	74.416	28.041	99.895	57.435	12.151	90.000	57.955
FaktorV	1.936	1.089	0.679	1.305	0.490	0.795	1.982	0.462	0.725
RMSE	0.133	0.137	1.283	0.115	0.506	0.922	0.794	0.980	0.629

Table 3-3 presents the results of the calibration for Driver D over various speed ranges. Like the other two drivers' results, the BX and EX terms show smaller variance than the other parameters. The null acceleration values show a different trend than the other two drivers. The results indicate in which speed ranges the drivers will exhibit more aggressive accelerations and decelerations and also in which speed ranges the driver will exhibit more relaxed accelerations and decelerations. The results also indicate that the trends in the null acceleration across the various speed ranges are driver dependent.

Table 3-3: Driver D Wiedemann Parameter Results

	20-30 kph	30-40 kph	40-50 kph	50-60 kph	60-70 kph	70-80 kph	80-90 kph	90-100 kph	100-110 kph
Ln-1	4.747	4.112	4.743	4.076	5.052	4.986	5.701	4.806	5.054
AXadd	6.592	6.000	5.734	8.705	8.549	9.679	8.151	3.715	1.000
BX	4.389	3.342	3.581	4.788	4.998	4.774	3.122	4.101	3.275
EX	2.753	3.251	2.963	2.983	2.930	2.621	2.517	2.739	2.940
CX	48.743	48.763	27.609	46.141	59.033	55.854	45.669	44.379	74.059
CX2	27.831	80.644	60.011	44.203	58.049	26.043	59.661	45.238	94.902
CLDVCX	47.611	37.187	27.609	40.783	54.775	52.795	42.980	28.316	27.806
OPDV	-2.348	-5.076	-3.487	-2.255	-2.100	-3.838	-2.770	-4.859	-4.144
bnull	0.184	0.557	0.143	0.004	0.190	0.060	0.303	0.000	0.000
bmaxmult	0.465	0.142	0.056	0.123	0.111	0.401	0.396	0.278	0.178
FaktorVmult	0.359	0.077	0.347	0.051	0.229	0.313	0.316	0.268	0.500
bminadd	-38.648	-32.517	-23.920	-22.070	-22.940	-30.448	-13.202	-30.814	-32.488
bminmult	0.318	0.186	0.185	0.299	0.311	0.138	0.075	0.183	0.277
Vdes	12.514	35.848	32.899	53.689	57.280	87.418	27.713	102.450	78.647
FaktorV	1.787	1.106	1.131	0.755	0.750	0.551	1.266	0.467	0.674
RMSE	0.843	0.618	0.253	0.274	0.249	0.368	0.928	0.820	0.694

With a bnull value of zero or close to zero, the SDV2 and OPDV thresholds become insignificant because there is no change in acceleration or speed made when crossing either threshold. In this situation, the governing thresholds are ABX and SDX, the minimum and maximum following distance thresholds. This means that the driver will either decelerate in the emergency regime or accelerate in the free driving regime. Table 3-4 presents the Root Mean Squared Error of the calibration for each driver over the speed ranges. The values shown are all below 1.5 which suggests that the results of the calibration create a relatively low error. Table 3-4 also shows that the calibration within each speed range appears to be dependent on the driver.

Table 3-4: Root Mean Squared Error by Driver and Speed Range

	20-30 kph	30-40 kph	40-50 kph	50-60 kph	60-70 kph	70-80 kph	80-90 kph	90-100 kph	100-110 kph
Driver B	0.9046	1.0670	0.8629	0.8207	1.1770	0.6392	0.8074	0.7186	0.5762
Driver C	0.1331	0.1365	1.2826	0.1145	0.5063	0.9216	0.7938	0.9797	0.6291
Driver D	0.8433	0.6181	0.2525	0.2742	0.2493	0.3677	0.9276	0.8199	0.6941

Table 3-5 shows the mean and standard deviation of the individual terms by driver. This table is the result of collapsing the different speed ranges in order to see the variability of each supposed constant. The results show that some of the terms have a high standard deviation while other terms have a smaller standard deviation. The terms with the lower standard deviation suggest that using a constant in their stead, as the original model suggests, would incur little error. On the other hand, using a constant in the stead of the terms with a high standard deviation would incur a large amount of error. For example, the terms CX, CX2, CLDVCX, and Vdes all have a large standard deviation which means that these terms cannot be considered a constant for the aforementioned reason.

Table 3-5: Average and Standard Deviation of Terms by Driver

	Average			Standard Deviation		
	Driver B	Driver C	Driver D	Driver B	Driver C	Driver D
Ln-1	5.22	4.63	4.81	0.591	0.687	0.497
AXadd	7.67	6.90	6.46	1.933	3.001	2.755
BX	3.93	3.99	4.04	0.353	0.594	0.730
EX	3.28	3.04	2.86	0.380	0.441	0.221
CX	53.76	62.97	50.03	32.927	26.327	12.572
CX2	61.43	61.89	55.18	23.182	20.455	22.622
CLDVCX	40.66	43.96	39.98	23.683	16.354	10.584
OPDV	-3.46	-3.62	-3.43	1.812	0.904	1.128
bnull	0.13	0.34	0.16	0.069	0.375	0.182
bmaxmult	0.22	0.24	0.24	0.133	0.125	0.150
FaktorVmult	0.23	0.25	0.27	0.111	0.132	0.140
bminadd	-28.36	-20.75	-27.45	18.489	7.456	7.595
bminmult	0.22	0.21	0.22	0.106	0.126	0.086
Vdes	65.77	52.71	54.27	34.736	31.283	30.143
FaktorV	0.85	1.05	0.94	0.475	0.580	0.419
RMSE	0.84	0.61	0.56	0.192	0.423	0.277

Figure 3-2 presents the AX thresholds for the three drivers over the speed ranges. The AX threshold represents the desired distance between stationary vehicles, but this value is used in the equations to calculate other thresholds and parameters. The figures show that this value is different for the speed ranges which mean that this parameter, in effect, includes some differences due to speed. This parameter should be a constant, but as the results show it is not and thus any of the equations that use this parameter will be different over the various speed ranges. This one parameter is used in the calculations for all of the thresholds and the closing deceleration.

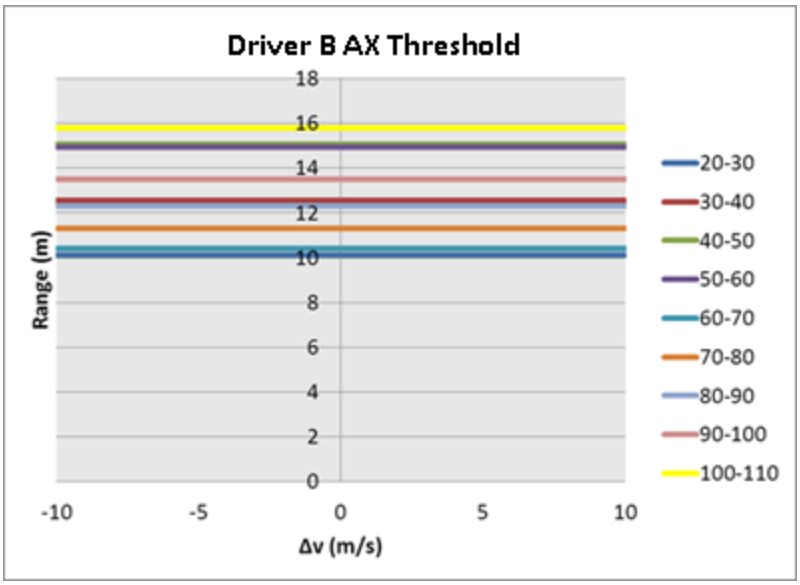

a) Driver B Ax Threshold

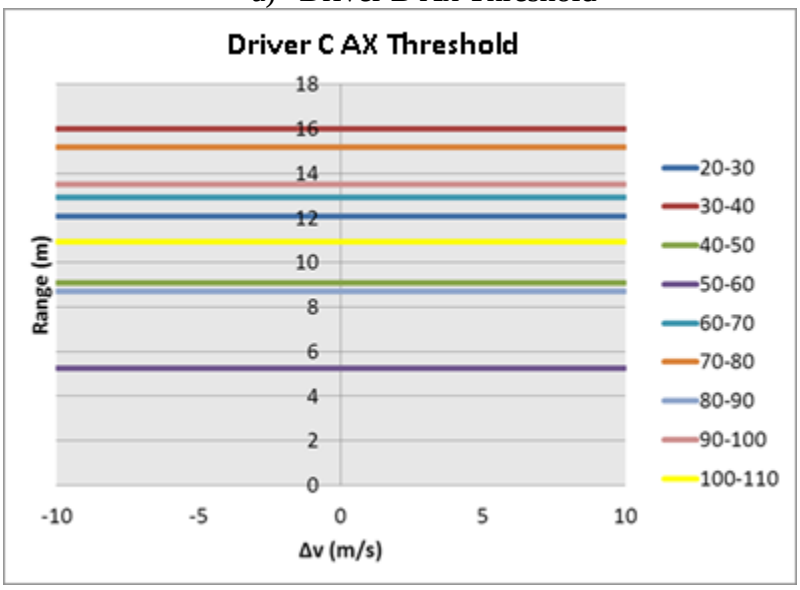

b) Driver C Ax Threshold

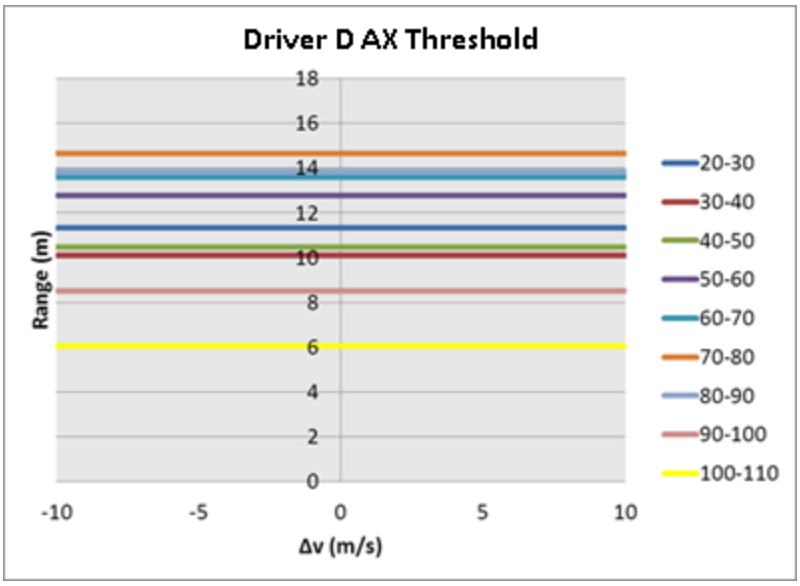

c) Driver D Ax Threshold

Figure 3-2: Driver AX Thresholds over the speed ranges

Figure 3-3 shows the ABX or minimum desired following distance thresholds for the three drivers. The threshold for Driver B shows a trend of increasing as the speed increases. The threshold for Driver D shows an increase as the speed increases until the 70-80 kph range then the threshold decreases as the speed increases. This indicates that the driver is more aggressive at the higher speed, speeds above 80 kph. Driver C shows this same aggressive behavior but in a different way. Driver C shows a sudden decrease in the ABX threshold from the 70-80 kph speed range to the 80-90 kph speed range, but from there, the threshold increases as the speed increases. This means that Driver C shows a jump in aggressiveness, but then decreasing aggression in response to higher speeds.

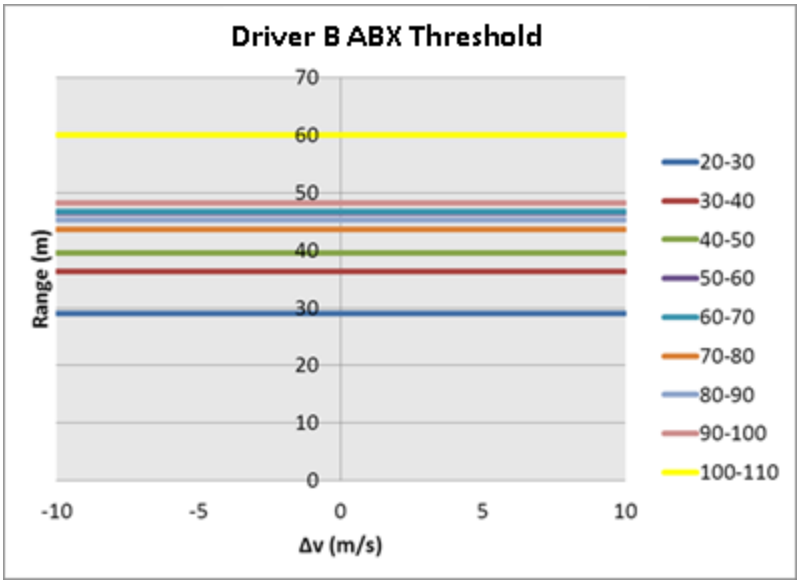

a) Driver B ABX Threshold

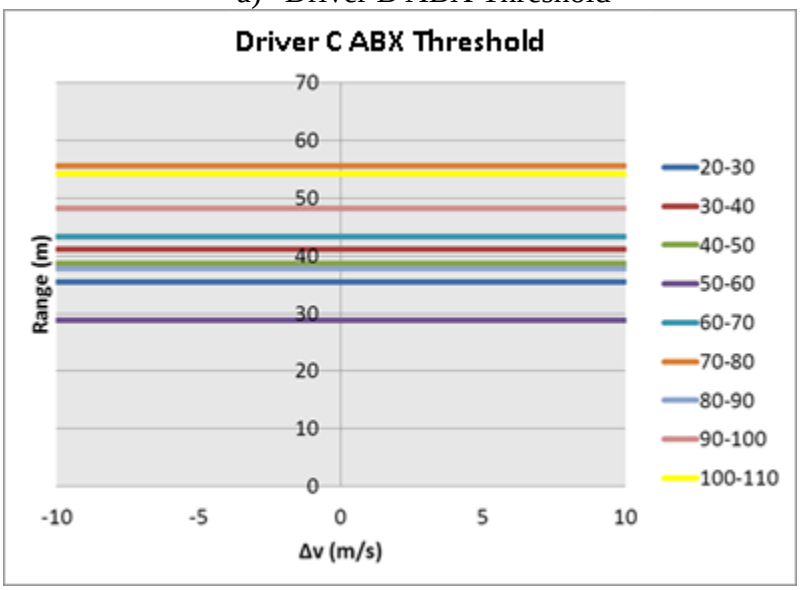

b) Driver C ABX Threshold

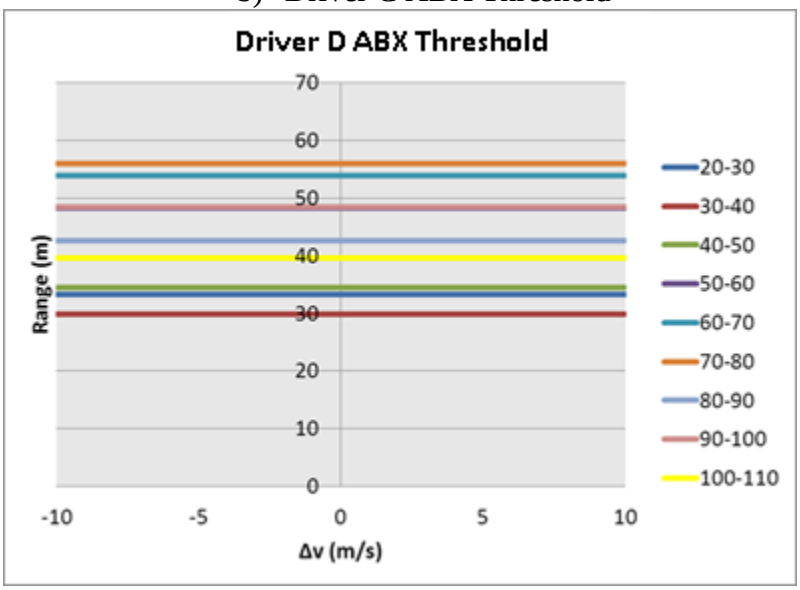

c) Driver D ABX Threshold

Figure 3-3: Driver ABX Thresholds over the speed ranges

Figure 3-4 shows the SDX or maximum desired following distance thresholds for the three drivers over the speed ranges. Driver B shows an increasing maximum desired following distance as the speeds increase up to the 60-70 kph speed range. Then, the threshold decreases by 40 meters and restarts the same increasing trend as the speed increases. The 100-110 kph threshold is far above the others which indicates that at these speeds the following regime is very large and thus the following regime can accurately represent the car following interactions. The maximum desired following distance for Driver C shows more of a clustering behavior than the thresholds for Driver B. The 70-

80 kph, 90-100 kph, and 100-110 kph thresholds are not included in the cluster, but these represent speeds at which Driver C shows car following behavior at greater distances. The maximum desired following distance for Driver D shows the same increase and decrease trend that was shown in the minimum desired following distance, ABX.

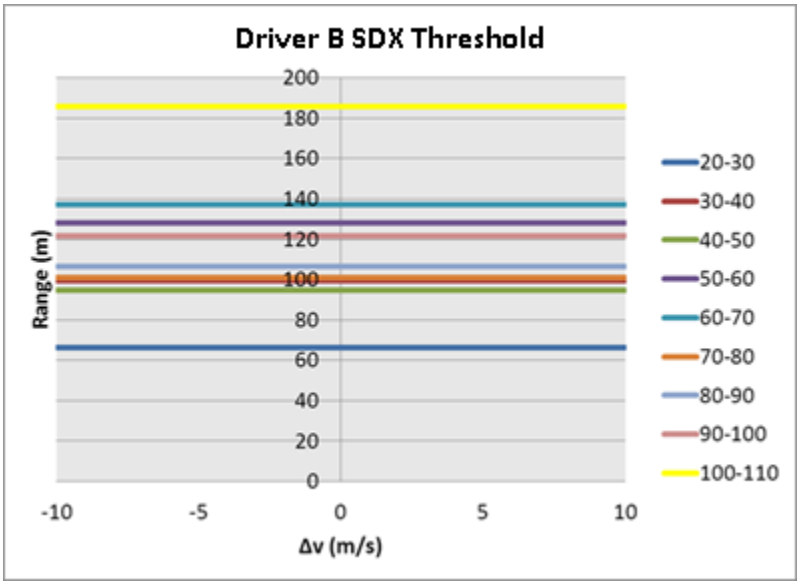

a) Driver B SDX Threshold

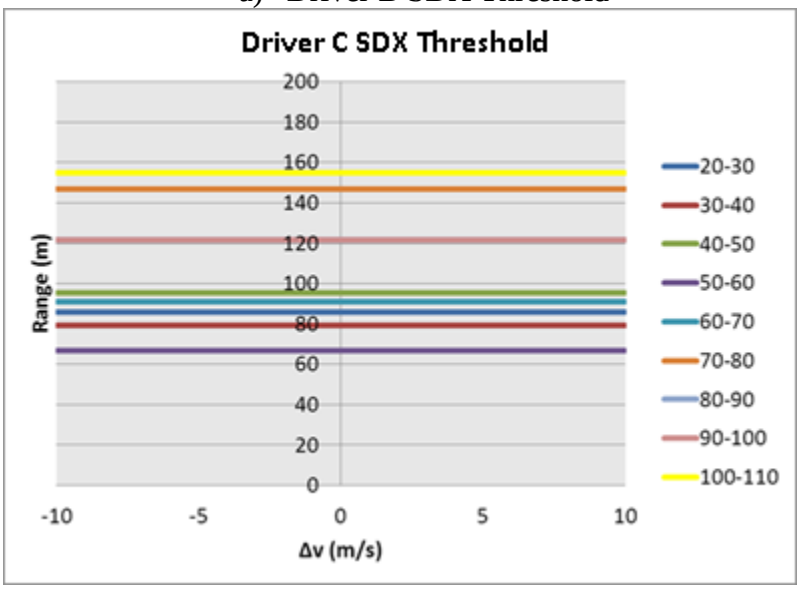

b) Driver C SDX Threshold

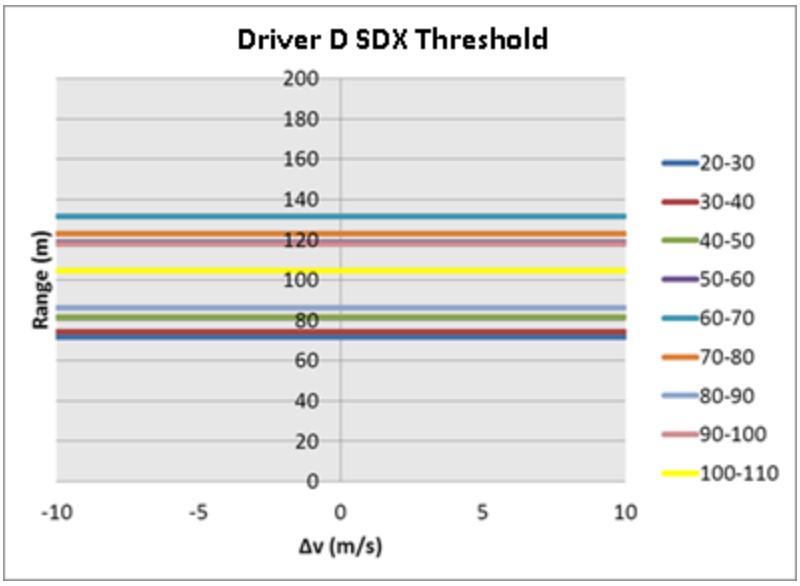

c) Driver D SDX Threshold

Figure 3-4: Driver SDX Thresholds over the speed ranges

Figure 3-5 shows the SDV or approaching point thresholds for the three drivers over the speed ranges. Driver B shows two clusters in the SDV threshold; one with speeds up to 50 kph and the second with speeds from 50 to 90 kph. Driver C has approaching point thresholds that begin with the lowest speed as the highest and then it decreases as the speed increases until 60 kph then it increases as the speed increases. The lower thresholds indicate that an approaching regime is not necessary at those speeds as the driver will directly enter the following regime. The thresholds in the middle indicate that an approaching regime is necessary for large speed differences, but at low speed differences, the driver will directly enter the following regime. The high thresholds indicate a necessary approaching regime except for very low speed differences.

A video reduction of a sample of the car following periods in the higher speed ranges revealed an interesting behavior in Driver B as compared to the other drivers. For the 100-110 kilometer per hour speed range, Driver B tended to approach the lead vehicles and then "settle in" and maintain that headway. This maintenance of the same headway requires Driver B to tap the brakes, lightly accelerate, and hold the clutch in a very active state. The 90-100 kilometer per hour speed range for Driver B exhibited similar behavior along with regular interaction with the lead vehicle or oscillation behavior which explains the "misplaced" SDV thresholds in Figure 3-5 as the two different behaviors will average out. Driver D, in the 100-110 kilometer per hour speed range, showed regular interaction with the lead vehicle which agrees with Figure 3-4. That agrees with the figure because with a higher speed and the same reaction time, the reaction distance needed will be greater for high speeds than low speeds.

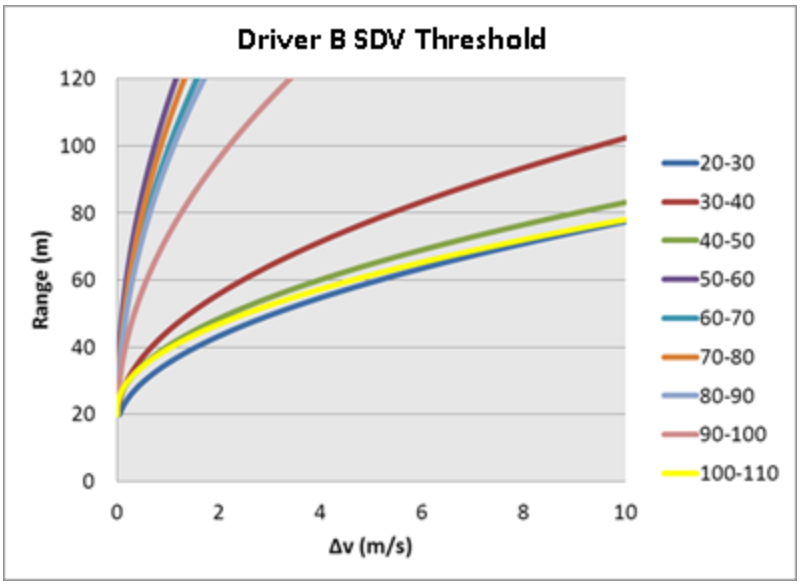

a) Driver B SDV Threshold

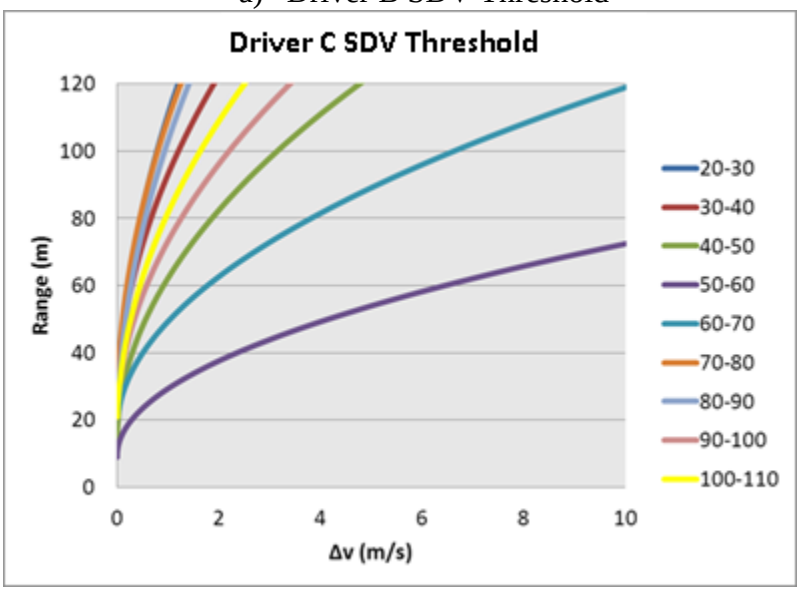

b) Driver C SDV Threshold

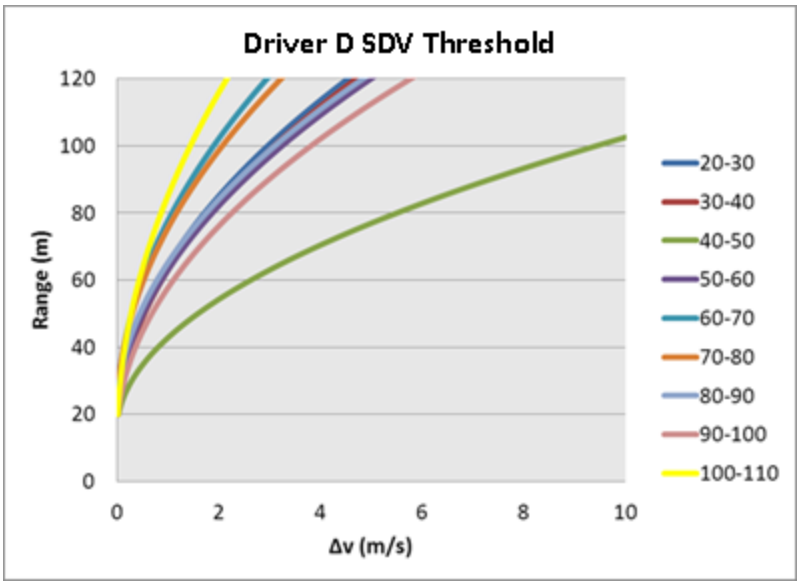

c) Driver D SDV Threshold

Figure 3-5: Driver SDV Thresholds over the speed ranges

Figure 3-6 shows the positive speed difference boundary or threshold to the following regime for the three drivers over the speed ranges. The thresholds for Driver B show two clusters; the high cluster causes a smaller following regime which indicates smaller oscillations while the lower cluster causes a larger following regime indicating larger oscillations. The speeds with larger oscillations are speeds 70-100 kph which means that at those speeds Driver B will wait to react until the speed difference between him and the lead vehicle is greater than at other speeds. This can almost indicate a more relaxed or distracted behavior.

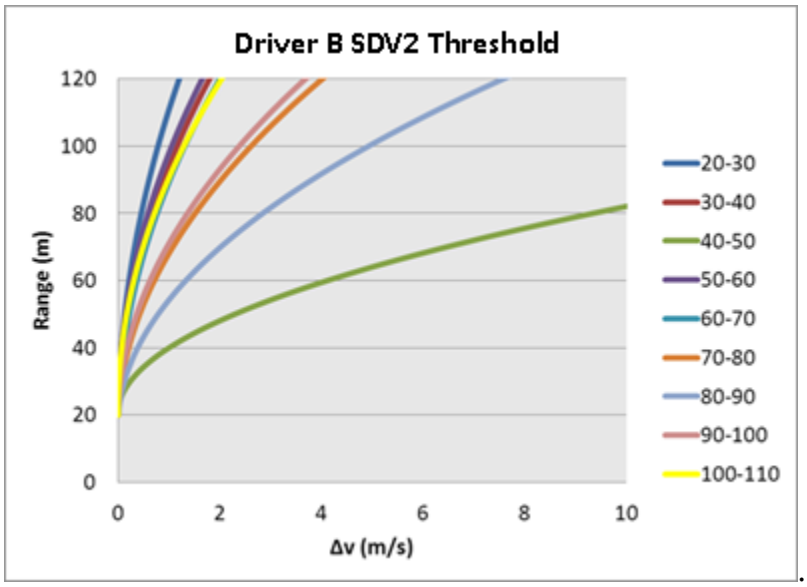

a) Driver B SDV2 Threshold

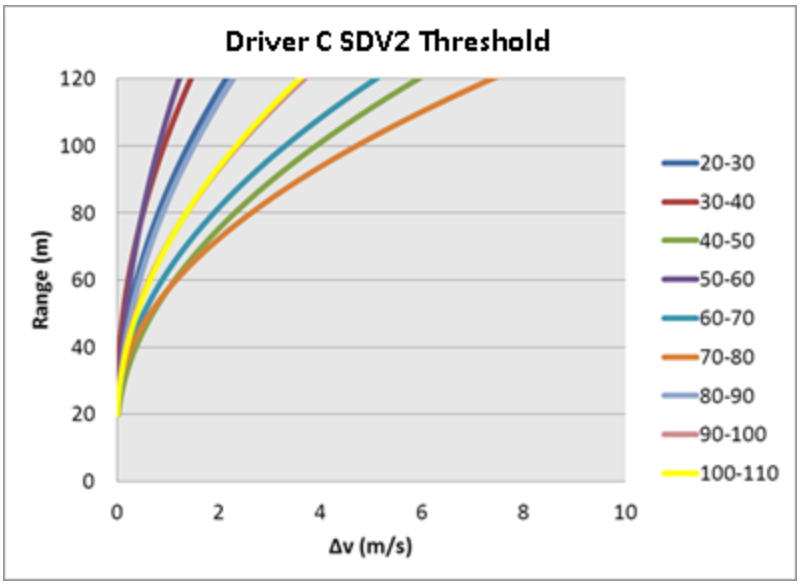

b) Driver C SDV2 Threshold

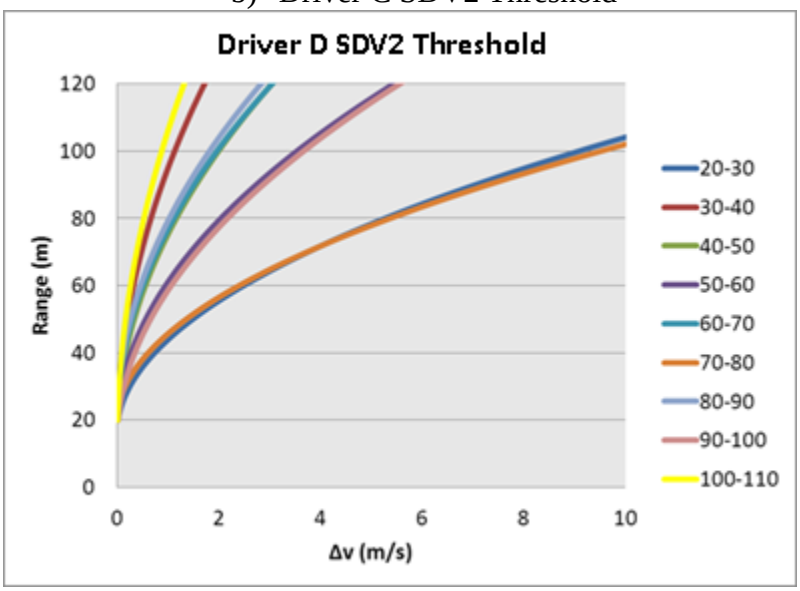

c) Driver D SDV2 Threshold

Figure 3-6: Driver SDV2 Thresholds over the speed ranges

Figure 3-7 presents the negative speed difference threshold (OPDV) or boundary to the following regime for the three drivers over the speed ranges. All of the thresholds in Figure 3-7 show a relaxed or low value as compared to the positive speed difference threshold. This shows that the drivers tend to be more responsive when approaching a lead vehicle than when falling behind a lead vehicle. Drivers C and D exhibit a clustering behavior in the OPDV thresholds, while Driver B shows more of a spread behavior. The OPDV thresholds for Driver B show an increase as the speed increases until the 70-80 kph speed range. Then, the OPDV thresholds decrease as the speed increases. The clustering of the thresholds in Driver C and D in Figure 3-7 indicates at

which speeds the drivers are more or less responsive to falling behind the lead vehicle. The low OPDV thresholds indicate less responsive while the high thresholds indicate more responsive behavior.

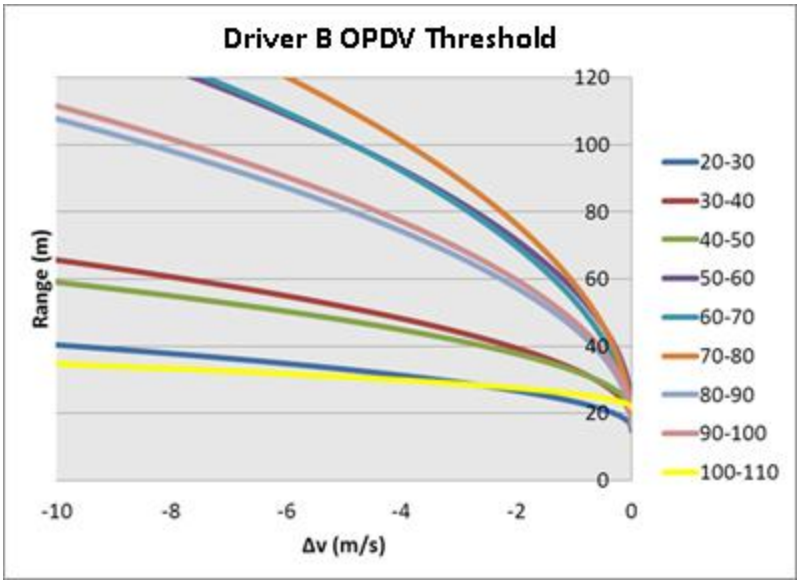

a) Driver B OPDV Threshold

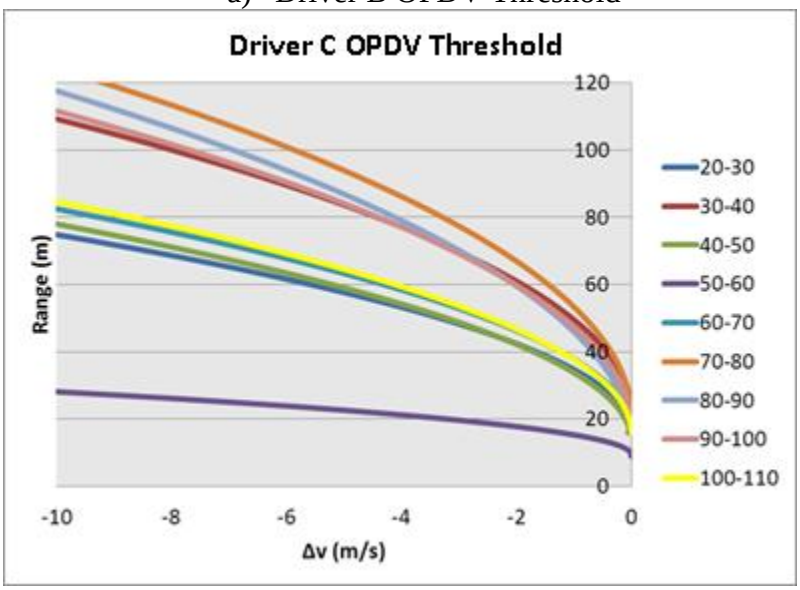

b) Driver C OPDV Threshold

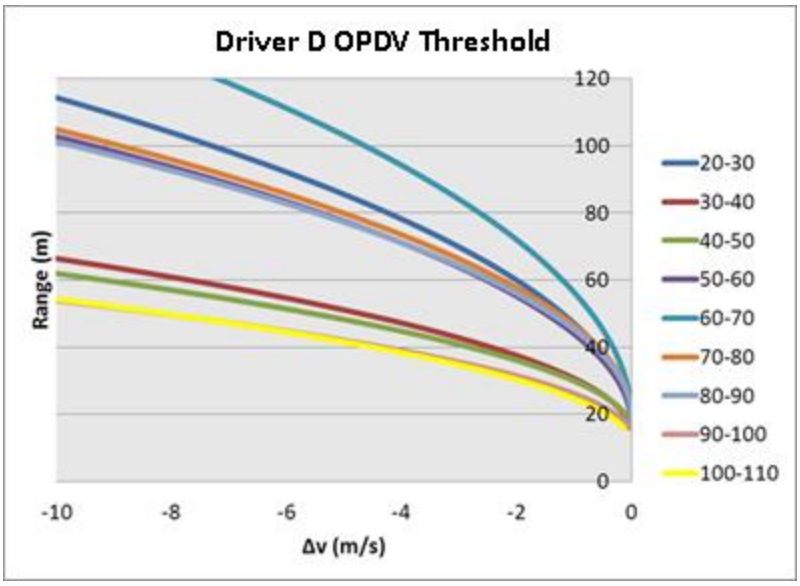

c) Driver D OPDV Threshold

Figure 3-7: Driver OPDV Thresholds over the speed ranges

3.6 Conclusions

The results show that the thresholds of the Wiedemann model vary over the speed ranges. This variation seems to be dependent upon the driver and thus driver profiles should be used instead of a single parameter. The null acceleration also shows variance over the speed ranges that seem to be driver dependent. The OPDV and SDV2 thresholds show that the drivers are more responsive to approaching than falling behind a lead vehicle. The variances also show at which speeds each driver exhibits aggressive behavior which adds value to the model. The inclusion of different aggression behavior for different speeds will only improve the Wiedemann model and make it a more realistic mimicry of the real world. As far as simulation packages are concerned, the inclusion of the ability to change the parameters according to the speed of the vehicle would serve to increase the accuracy of simulations. Future research is recommended in the development and implementation of driver aggression profiles in the Wiedemann model. Also, discovering ways to group drivers according to their profiles would potentially reduce the number of profiles needed in order to gain a more accurate simulation of traffic flow.

Acknowledgment

This material is based upon work supported by the Federal Highway Administration under Agreement No. DTFH61-09-H-00007. Any opinions, findings, and conclusions or recommendations expressed in this publication are those of the Author(s) and do not necessarily reflect the view of the Federal Highway Administration.

The authors would like to express thanks to Dr. C.Y. David Yang, the FHWA Agreement Manager, for his continued support and guidance during this project. They would also like to thank individuals at Virginia Tech and the Virginia Tech Transportation Institute who contributed to the study in various ways: Greg Fitch, Shane McLaughlin, Kelly Stanley and Rebecca Olson.

References

1. Wiedemann, R., *Simulation des Strassenverkehrsflusses.* Schriftenreihe des Instituts für Verkehrswesen der Universität Karlsruhe, Band 8, Karlsruhe, Germany. 1974.
2. PTV-AG, *VISSIM 5.10 User Manual.* 2008.
3. Olson, R., et al., *DRIVER DISTRACTION IN COMMERCIAL VEHICLE OPERATIONS.* 2009, Center for Truck and Bus Safety; Virginia Tech Transportation Institute: Blacksburg VA. p. 285.
4. Ranjitkar, P. and T. Nakatsuji, *A TRAJECTORY BASED ANALYSIS OF DRIVERS' RESPONSE IN CAR FOLLOWING SITUATIONS.* TRB 2010 Annual Meeting CD-ROM, 2010: p. 21.
5. Ossen, S. and S.P. Hoogendoorn, *Validity of trajectory-based calibration approach of car-following models in presence of measurement errors.* Transportation Research Record, 2008(2088): p. 117-125.
6. Brackstone, M., *Driver Psychological Types and Car Following:Is There a Correlation? Results of a Pilot Study*. 2003. p. 6.
7. Schultz, G.G. and L.R. Rilett, *Analysis of Distribution and Calibration of Car-Following Sensitivity Parameters in Microscopic Traffic Simulation Models.* 2004: p. 11.
8. Panwai, S. and H. Dia, *Comparative evaluation of microscopic car-following behavior.* IEEE TRANSACTIONS ON INTELLIGENT TRANSPORTATION SYSTEMS, 2005. **6**(3): p. 314-325.
9. Siuhi, S. and M. Kaseko, *PARAMETRIC STUDY OF STIMULUS-RESPONSE BEHAVIOR FOR CAR-FOLLOWING MODELS.* TRB 2010 Annual Meeting CD-ROM, 2010.
10. Osaki, H., *Reaction and anticipation in the Car-Following Behavior.* In Proceedings of the 12 International Symposium on the Theory of Traffic Flow and Transportation, 1993.
11. Subranmanian, H., *Estimation of Car-Following Models.* Master Thesis, 1996.
12. Ahmed, K.I., *Modeling Drivers' Acceleration and Lane Changing Behavior.* PhD Dissertation, 1999.
13. Toledo, T., *Integrating Driving Behavior.* PhD Dissertation,, 2003.
14. Menneni, S., C.P.D. Sun, P.E., and P. Vortisch, *An Integrated Microscopic and Macroscopic Calibration for Psycho-Physical Car Following Models* TRB 2009 Annual Meeting CD-ROM 2008: p. 17.
15. Hoogendoorn, S. and R. Hoogendoorn, *A Generic Calibration Framework for Joint Estimation of Car Following Models using Microscopic Data.* TRB 2010 Annual Meeting CD-ROM, 2010: p. 17.

4. RECONSTRUCTING THE WIEDEMANN MODEL USING NATURALISTIC DRIVING DATA[3]

Abstract
This research effort reconstructs the Wiedemann car-following model for truck driver behavior using the Naturalistic Truck Driving Study's (NTDS) conducted by Virginia Tech Transportation Institute. This Naturalistic data was collected by equipping 9 trucks with various sensors and a data acquisition system. The equipment included accelerometers, radar, and vehicle network's existing sensors. The specific variables of interest in the Wiedemann model were the range and range-rate obtained from the radar. The data for four different drivers was selected for analysis. When looking at the equations for the Wiedemann model with a specific driver in mind, the perspective changes and thus the form of the equations change. These equations have driver specific calibrated parameters as opposed to generic calibration parameters with driver specific random numbers. This makes the model more specific to individual drivers with heterogeneity being created by using the driver specific calibration parameters for multiple drivers. The results show drastic differences between the drivers which supports the idea that the modeling car-following behavior needs to be more driver specific than generic. The Wiedemann model currently only considers car-following cases where the subject vehicle approaches the lead vehicle at a higher speed. As seen in the naturalistic data, there is a sizable amount of cases where a lead vehicle merges in front of the subject vehicle which causes the subject vehicle to accelerate and follow. This behavior was addressed by the addition of another threshold to the Wiedemann model. This threshold provides clarity for where the decision to "hook" onto a lead vehicle is made. The naturalistic data also provided data for when a pass maneuver was executed or the subject vehicle decided to follow. The addition of a pass threshold allows pass decision logic to be represented in the same framework as car-following logic and thus the transition between the two is smoothed. The addition of the new thresholds and adjustment of the equation to be driver specific adds value to the Wiedemann model by being more inclusive of "real world" driver behavior.

[3] Paper has been published in the proceedings of the TRB Traffic Flow Theory Summer Meeting and Conference, Annecy, France

4.1 Introduction

Several studies have tried to incorporate driver behavior or to classify driver's attributes, however, direct correlation with real driving variables is rare and parameterization of objective behavior is still in its development. Some studies have been limited to very controlled experiments, recent ones have used aerial photography based measurement from helicopters(Ranjitkar and Nakatsuji, 2010), GPS data, test track data and trajectory data form NGSIM

Ossen and Hoogendoorn (Ossen and Hoogendoorn, 2008) studied the car-following behavior of individual drivers using vehicle trajectory data that were extracted from high-resolution digital images collected at a high frequency from a helicopter. The analysis was performed by estimating the parameters of different specifications of the GHR car-following rule for individual drivers. In 80 % of the cases, a statistical relation between stimuli and response could be established. The Gipps (a safe distance model) and Tampere (stimulus-response model) models and a synthetic data based approach were used for assessing the impact of measurement errors on calibration results. According to the authors, the main contribution of their study was that considerable differences between the car-following behaviors of individual drivers were identified that can be expressed in terms of different optimal parameters and also as different car-following models that appear to be optimal based on the individual driver data. This is an important result taking into account that in most models a single car-following rule is used. The authors also proposed for future research to apply more advanced statistical methods and to use larger databases. Brackstone (Brackstone, 2003) using data collected with an instrumented vehicle that was assembled at TRG Southampton parameterize the Wiedeann's threshold for a typical following spiral. As a result they represent the action points as a function of a probability distribution based on ground speed.

Micro-simulation software packages use a variety of car-following models including Gipps' (AIMSUN, SISTM, and DRACULA), Wiedemann's (VISSIM), Pipe's (CORSIM), and Fritzsche's (PARAMICS). And different automated calibration parameters such as genetic algorithms have been used to calibrate the distribution of car-following sensitivity parameters *(Schultz and Rilett, 2004)*. Panwai and Dia (Panwai and Dia, 2005) compared the car-following models between different simulation software, including AIMSUN, PARAMICS and VISSIM using an instrumented vehicle to record differences in speed and headway (Leading speed, relative distance, relative speed, follower acceleration were recorded.) The EM shows similar values for psychophysical models in VISSIM and PARAMICS and lower values in AIMSUN. The Root Mean Square Error and qualitative drift and goal-seeking analyses also showed a substantially different car-following behavior for PARAMICS. . Siuhi and Kaseko (Siuhi and Kaseko, 2010) demonstrated the needs for separate models for acceleration and deceleration responses by developing a family of car-following models and addressing the shortcomings of the GM model. Previous work from Osaki (Osaki, 1993) and Subranmanian (Subranmanian, 1996) modified the GM model separating the acceleration and deceleration responses. Ahmed (Ahmed, 1999), following some work from Subranmanian assumed non linearity in the stimulus term and introduced traffic density. Results from Ahmed (Ahmed, 1999) and Toledo (Toledo, 2003) showed , against popular belief, that acceleration increases with speed but decreases with vehicle separation. Due to statistical insignificance, Ahmed and Toledo also removed speed from their deceleration models. Siuhi and Kasvo (Siuhi and Kaseko, 2010) addressed some of these shortcomings by developing separate models, not only for acceleration and deceleration, but also for steady-state responses. Nonlinear regression with robust standard errors was used to estimate the model parameters and obtain the distributions across drivers. The stimulus response thresholds that delimit the acceleration and deceleration responses were determined based on signal detection theory.

Schultz and Rilett (Schultz and Rilett, 2004) proposed a methodology which introduces and calibrates a low parameter distribution using measures of central tendency and dispersion to generate input parameters for car-following sensitivity factors in simulation models using CORSIM. Ten different car-following sensitivity factors were identified to determine the distribution of desired car-following distance and both lognormal and normal distributions were considered under the condition that car-following sensitivity factors fall within range. The results showed that with automated calibration method such as genetic algorithm, the mean absolute error between simulated and observed traffic volume can be minimized.

Using two models of similar complexity (number of parameters): the "Intelligent Driver Model" (IDM) and the "Velocity Difference Model" (VDIFF), Kesting and Treiber (Kesting and Treiber, 2008) researched car-following behaviors on individual drivers using publicly available trajectory data for a straight one-lane road in Stuttgart, Germany. They used a nonlinear optimization procedure based on a genetic algorithm to minimize the deviations between the observed driving dynamics and the simulated trajectory. One of the major findings of the study was that a significant part of the deviations between measured and simulated trajectories can be attributed to the inter-driver variability and the intra-driver variability (stipulating that human drivers do not drive constantly over time, and their behavioral driving parameters change)—the later accounts for a large part of the deviations between simulations and empirical observations.

Menneni et al (Menneni et al., 2008) presented a calibration methodology of the VISSIM Wiedemann car-following model based on integrated use of microscopic and macroscopic data using NGSIM Relative distance vs. relative speed graphs were used for the microscopic calibration, specifically to determine the action points (it is important to notice that action points were not identical to perception threshold). Scatter and distribution of action points on relative distance versus relative velocity graphs also showed similarity in driver behavior between the two freeways.

Hoogendoorn and Hoogendoorn (Hoogendoorn and Hoogendoorn, 2010) proposed a generic calibration framework for joint estimation of car following models. The method employed relies on the generic form of most models and weights each model based on its complexity. This new approach can cross-compare models of varying complexity and even use multiple trajectories when individual trajectory data is scarce. Prior information can also be used to realistically estimate parameter values.

4.2 Wiedemann Car-Following Model

The Wiedemann car-following model was originally formulated in 1974 by Rainer Wiedemann (Wiedemann, 1974) . This model is known for its extensive use in the microscopic multi-modal traffic flow simulation software, VISSIM (PTV-AG, 2008). The Wiedemann model was constructed based on conceptual development and limited available data, and has to be calibrated to specific traffic stream data.

The principal ideas behind the Wiedemann model were used in this paper, but the exact shape or formula used in the model are updated using the Naturalistic data that is deemed to be the best available source of "real world" data.

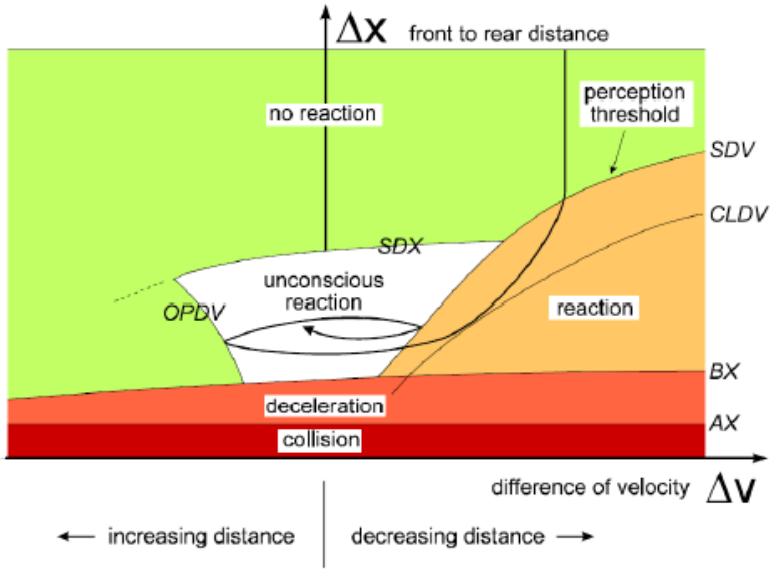

Figure 4-1: Wiedemann 74 Car Following Logic(PTV-AG, 2008)

Figure 4-1 shows the graphical form of the Wiedemann 74 model. The different thresholds are shown with a certain shape that can only be amplified during the calibration procedure. The figure shows the subject vehicle approaching a lead vehicle (ΔX decreasing due to higher subject vehicle's speed shown by a positive ΔV), and entering a perception area (crossing the SDV threshold) where it has to reduce speed. The subject vehicle then crosses another threshold (CLDV) where it reacts and reduces speed even further to enter an unconscious reaction car-following episode. The subject vehicle then continues the unconscious car-following episode as long as it remains bounded by the OPDV, SDX, and SDV thresholds.

4.3 Naturalistic Data

Introduction to Naturalistic Data

As opposed to traditional epidemiological and experimental / empirical approaches, this *in situ* process uses drivers who operate vehicles that have been equipped with specialized sensor, processing, and recording equipment. In effect, the vehicle becomes the data collection device. The drivers operate and interact with these vehicles during their normal driving routines while the data collection equipment is continuously recording numerous items of interest during the entire driving. Naturalistic data collection methods require a sophisticated network of sensor, processing, and recording systems. This system provides a diverse collection of both on-road driving and driver (participant, non-driving) data, including measures such as driver input and performance (e.g., lane position, headway, etc.), four camera video views, and driver activity data. This information may be supplemented by subjective data, such as questionnaire data.

As part of the NTDS study(Olson et al., 2009) four companies and 100 drivers participated in this study. Each participant in this on-road study was observed for approximately 4 consecutive work weeks. One hundred participants were recruited from four different trucking fleets across seven terminals and one to three trucks at each trucking fleet were instrumented (nine trucks total). After a participant finished 4 consecutive weeks of data collection, another participant started driving the instrumented truck. Three forms of data were collected by the NTDS DAS: video, dynamic performance, and audio. Approximately

14,500 driving-data hours covering 735,000 miles traveled were collected. Nine trucks were instrumented with the DAS.

The following is a typical description of how the data collection is performed, along with accompanying screenshots and information describing how the system works and how data can be used. Four cameras monitor and record the driver's face, forward road view, and left- and right-side of the tractor trailer, which are used to observe the traffic actions of other vehicles around the vehicle. Figure 4-2 displays the four camera views and approximate fields-of-view. Low-level infrared lighting (not visible to the driver) illuminates the vehicle cab so the driver's face and hands could be viewed via the camera during nighttime driving. The sensor data associated with the project were originally collected in a proprietary binary file format. A database schema was devised and the necessary tables were created. The schema preserves the organization of data into modules; i.e. all of the variables associated with a particular module are stored in one table in the database. The import process itself consisted of reading the binary files, writing the data to intermediate comma separated value (CSV) files and "bulk inserting" the CSV files into the database. A stored procedure is available that allows one to query the database using the module and variable names rather than database table and column names.

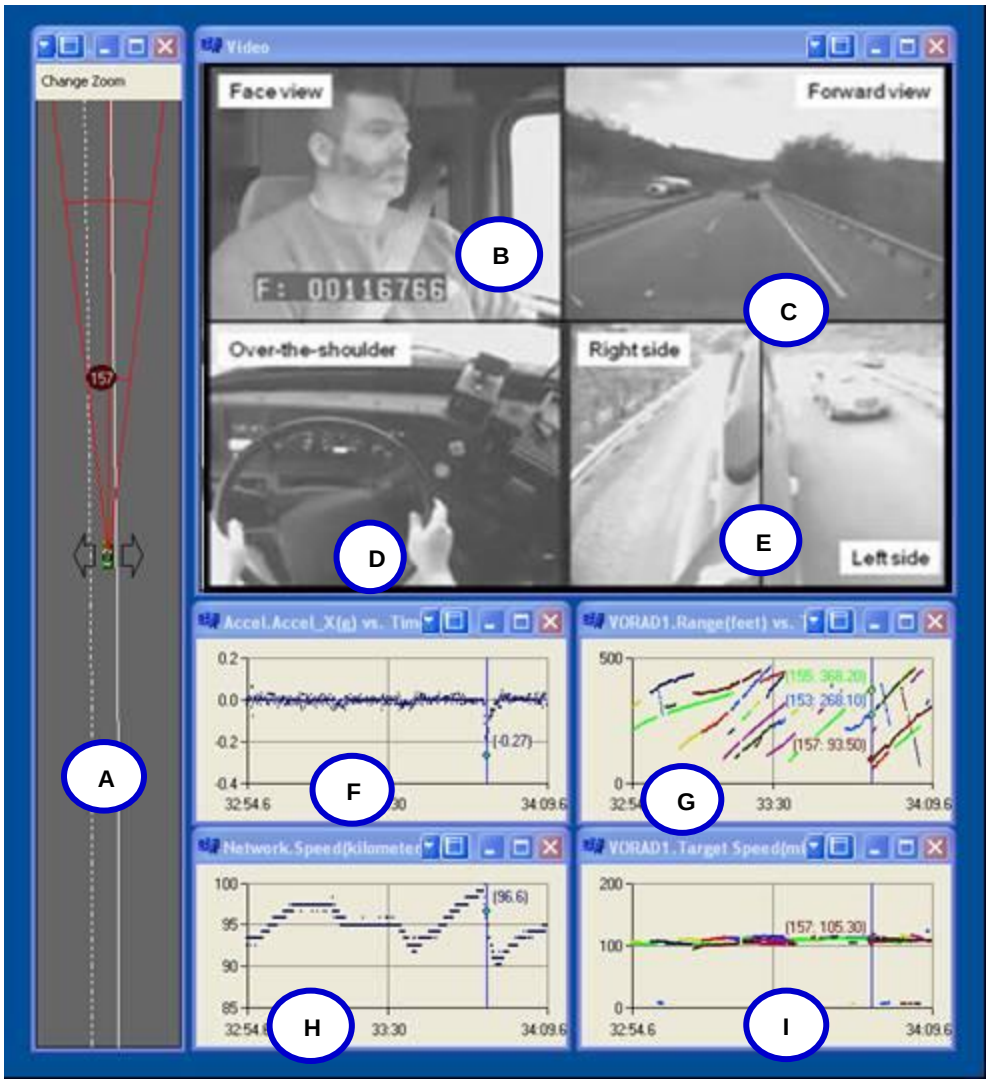

Figure 4-2: View of DAS Data

- **A** = Plan view of subject vehicle and road position based on Road Scout lane tracker.
- **B** = Video feed recording face shot of driver, with frame number, used to synchronize video and parametric data.
- **C** = Video feed recording forward view.
- **D** = Video feed recording of over-the-shoulder view of driver, which is used for determining driver distractions.
- **E** = Video feed recording both rear-left and rear-right images.
- **F** = Data feed from X/Y Acceleration sensor indicating longitudinal acceleration as measured in "g's" (g's are the range to primary target as determined by VORAD).
- **G** = Data feed from Front VORAD Sensor indicating range to primary target as determined by VORAD versus Time.
- **H** = Network speed is the vehicle's speed.
- **I** = Data feed showing VORAD Primary Target Closing Rate (WRT subject vehicle

Car following automatic extraction

Car-following situations were automatically extracted from the enormous volume of driving data in the database in order to analyze the car following driver behavior. The filtering process is an iterative process where initial values and conditions are used and after the events are flagged they are reviewed in the video data to adjust the values accordingly in order to obtain minimum noise. Visual inspection of the first subsets created revealed some non-car following events so additional filtration was thus performed to remove these events from the database.

Specifically, car following periods were extracted automatically according to these conditions:

- Radar Target ID>0

  This eliminates the points in time without a radar target detected

- Radar Range<=400ft

  This represents four seconds of headway at 70 mph

- -6.25ft<Range*Sin (Azimuth) <6.25ft

  This restricts the data to only one lane in front of the lead vehicle

- Speed>=20km/h

  This speed was used in order to minimize the effect of traffic jams, but still leave the influence of congestion in the data

- Rho-inverse <=1/2000

  This limits the curvature of the roadway such that vehicles are not misidentified as being in the same lane as the subject vehicle when roadway curvature is present.

- Length of car following period >= 30 seconds

The automatic extraction process was verified from a sample of events through video analysis. For the random sample of 400 periods, 392 were valid car following periods. Therefore, the research team used the data that has been extracted automatically.

4.4 Reconstruction of The Wiedemann model

The reconstruction process employed has two main sections. The first section is the evaluation and adaptation of the Wiedemann model according to the naturalistic data. The second section is the addition of new thresholds that aim to represent recurrent phenomenon that were found in the naturalistic data.

Calibration and Adaptation of Existing Model

The Wiedemann model uses random numbers in order to create heterogeneous traffic stream behavior in VISSIM. These random numbers are meant to simulate behavior of different drivers. The naturalistic data is a perfect match for this situation because the data is collected for individual drivers. Data for four different drivers was selected and processed in order to reconstruct the Wiedemann car-following model.

The focus of the reconstruction began by analyzing the equations for the different thresholds and different accelerations. This coincided with the design of a calibration framework tailored specifically to the naturalistic data. The analyzed and adjusted equations were implemented into the calibration framework, a Microsoft Excel spreadsheet. Microsoft Excel 2010 was chosen for this task due to the new evolutionary algorithm included in Excel's Solver Add-in. The framework consisted of expressing the logic of the Wiedemann model as a series of state transitions. The states are defined by the different thresholds and each state has an equation or parameter for the acceleration. The optimization function was simply the minimization of the error between the values calculated in the Wiedemann model and the values directly from the data.

Desired Distance between Stationary Vehicles

The starting point for the Wiedemann model is the desired distance between stationary vehicles. The value calculated by Equation 4-1 is used in the calculations for the other thresholds. When analyzing Equation 4-1 with an individual driver in mind, the calibration parameters can be combined with the driver dependent random number in order to create a single calibration parameter as shown in Equation 4-2.

$$\boldsymbol{AX = L_{n-1} + AXadd + RND1_n * AXmult} \quad \textbf{(4-1)}$$

L_{n-1} is the length of the lead vehicle

$AXadd, AXmult$ are calibrated parameters

$RND1_n$ is a normally distributed driver dependent parameter

$$\boldsymbol{AX = L_{n-1} + AXadd} \quad \textbf{(4-2)}$$

The desired minimum following distance threshold is calculated using Equation 4-3 and Equation 4-4. The calibration parameters and random number can be combined to produce Equation 4-5.

$$\boldsymbol{ABX = AX + BX} \quad \textbf{(4-3)}$$

$$\boldsymbol{BX = (BXadd + BXmult * RND1_n) * \sqrt{v}} \quad \textbf{(4-4)}$$

$BXadd, BXmult$ are calibration parameters

v is the minimum of the speed of the subject vehicle and the lead vehicle

$$\boldsymbol{BX = BXmult * \sqrt{v}} \quad \textbf{(4-5)}$$

The maximum following distance is calculated using Equation 4-6 and Equation 4-7. Equation 4-7 includes calibration parameters and random numbers, but mainly serves as a multiplier to BX. Since it serves as only a multiplier Equation 4-7 can be condensed to Equation 4-8.

$$\boldsymbol{SDX = AX + EX * BX} \quad \textbf{(4-6)}$$

$$\boldsymbol{EX = EXadd + EXmult * (NRND - RND2_n)} \quad \textbf{(4-7)}$$

$EXadd, EXmult$ are calibration parameters.

$NRND$ is a normally distributed random number.

$RND2_n$ is a normally distributed driver dependent parameter.

$$\boldsymbol{EX = EXmult} \quad \textbf{(4-8)}$$

The Perception Threshold marks the point that a driver will begin to react to the lead vehicle. This threshold is calculated by the use of Equation 4-9.Equation 4-2 and Equation 4-10 are needed in order to calculate Equation 4-9.

$$\boldsymbol{SDV = \left(\frac{\Delta x - L_{n-1} - AX}{CX}\right)^2} \quad \textbf{(4-9)}$$

$$\boldsymbol{CX = CXconst * \left(CXadd + CXmult * \left(RND1_n + RND2_n\right)\right)} \quad \textbf{(4-10)}$$

L_{n-1} is the length of the lead vehicle. $CXconst, CXadd, CXmult$ are calibrated parameters. $RND1_n, RND2_n$ are normally distributed driver dependent parameters.

When looking at the equation with a specific driver in mind, the equations can be reduced by combining all of the variables that would have a constant value. This collapses the equation to be Equation 4-11.

$$\boldsymbol{CX = CX} \quad \textbf{(4-11)}$$

This collapses the equations to now only have one input variable and two calibrated parameters which are specific to a single driver.

The reaction curve marks the location of a second acceleration change point while still closing on the lead vehicle. In VISSIM this threshold is assumed to be equivalent to the Perception Threshold. Due to that similarity, the equation used for the Reaction Threshold, Equation 4-12 is derived from Equation 4-9.

$$\boldsymbol{CLDV = \left(\frac{\Delta x - L_{n-1} - AX}{CLDVCX}\right)^2} \quad \textbf{(4-12)}$$

$CLDVCX$ is a calibrated parameter specific to one driver

The OPDV (Opening Difference in Velocity) curve is primarily a boundary to the unconscious reaction region. It represents the point where the driver notices that the distance between his or her vehicle and the lead vehicle is increasing over time. When this realization is made the driver will accelerate in order to maintain desired space headway. This threshold is calculated using Equation 4-13.

$$\boldsymbol{OPDV = CLDV * (-OPDVadd - OPDVmult * NRND)} \quad \textbf{(4-13)}$$

$OPDVadd, OPDVmult$ are calibrated parameters

$NRND$ is a normally distributed random parameter

When considering only one driver, the equation changes to Equation 4-14.

$$\boldsymbol{OPDV = CLDV * OPDVmult} \quad \textbf{(4-14)}$$

The Wiedemann model reuses the Perception Threshold as a boundary to the unconscious reaction region. This would again be the point where the driver notices that the distance between his or her vehicle and the lead vehicle is decreasing over time, but this second use of the threshold is used when the subject vehicle is already engaged in following the lead vehicle. This reuse of the Perception Threshold was given its own equation in order to provide hysteresis control and to evaluate the adequacy of reusing the Perception threshold. Equation 4-15 is of the same form as Equation 4-9, but with a different calibrated parameter.

$$\boldsymbol{SDV2} = \left(\frac{\Delta x - \boldsymbol{L_{n-1}} - \boldsymbol{AX}}{\boldsymbol{CX2}}\right)^{\boldsymbol{2}} \quad \textbf{(4-15)}$$

$CX2$ is a calibrated parameter

The first state is the free driving regime where the subject vehicle is not reacting to a lead vehicle and is travelling at a desired speed or accelerating to a desired speed. The Free Driving Regime is defined as the area above the Perception Threshold and the Maximum Following Distance Threshold. If the subject vehicle enters the free driving regime, the subject vehicle will then accelerate until the desired speed is reached. The value for this acceleration is calculated using Equation 4-16 and Equation 4-17. Equation 4-16 relates the maximum speed to the current speed times Equation 4-17 and calculates an acceleration value accordingly in order to reach the maximum speed. Equation 4-18 is derived when the acceleration ends at the desired speed and not the maximum speed. Also, Equation 4-19 is derived from the fact that Equation 4-17 will reduce to a constant value.

$$\boldsymbol{b_{max}} = \boldsymbol{BMAXmult} * (\boldsymbol{v_{max}} - \boldsymbol{v} * \boldsymbol{FaktorV}) \quad \textbf{(4-16)}$$

$BMAXmult$is a calibration parameter

$v_{max}$is the maximum speed of the vehicle

$$\boldsymbol{FaktorV} = \frac{\boldsymbol{v_{max}}}{\boldsymbol{v_{des}} + \boldsymbol{FAKTORVmult} * (\boldsymbol{v_{max}} - \boldsymbol{v_{des}})} \quad \textbf{(4-17)}$$

$FAKTORVmult$ is a calibration parameter

$v_{des}$is the desired speed

$$\boldsymbol{b_{max}} = \boldsymbol{BMAXmult} * (\boldsymbol{v_{des}} - \boldsymbol{v} * \boldsymbol{FaktorV}) \quad \textbf{(4-18)}$$

$$\boldsymbol{FaktorV} = \boldsymbol{FAKTORVmult} \quad \textbf{(4-19)}$$

The approaching regime occurs when a vehicle in the Free Driving Regime passes the Perception Threshold. This vehicle will then decelerate according to Equation 4-20.

$$\boldsymbol{b_n} = \frac{\boldsymbol{1}}{\boldsymbol{2}} \frac{(\Delta)^{\boldsymbol{2}}}{\boldsymbol{ABX} - (\Delta \boldsymbol{x} - \boldsymbol{L_{n-1}})} + \boldsymbol{b_{n-1}} \quad \textbf{(4-20)}$$

The Closely Approaching regime occurs only when a vehicle in the approaching regime passes the Closing Difference in Velocity Threshold. In VISSIM this regime is ignored, so the deceleration is still calculated by Equation 4-20.

The Deceleration Following regime occurs as a result of a vehicle in the Approaching or Closely Approaching regime passes the Perception Threshold or a vehicle in the Acceleration Following Regime passes the Second Perception Threshold. When a vehicle enters the Deceleration Following regime the acceleration is calculated by the negative of Equation 4-21. When considering one driver Equation 4-21 can be reduced to Equation 4-22.

$$\boldsymbol{b_{null}} = \boldsymbol{BNULLmult} * (\boldsymbol{RND4_n} + \boldsymbol{NRND}) \quad \textbf{(4-21)}$$

$BNULLmult$is a calibration parameter

$RND4_n$is a normally distributed driver dependent parameter

$$b_{null} = b_{null} \quad \textbf{(4-22)}$$

The Acceleration following regime occurs when a vehicle in the Deceleration Following regime passes the Opening Difference in Velocity Threshold or a vehicle in the Emergency Regime passes the Minimum Following Distance Threshold. The acceleration for a vehicle in the Acceleration following regime is simply the positive value of Equation 4-21. If a vehicle in this regime accelerates and crosses the Maximum Following Distance Threshold, then that vehicle will enter the Free Driving regime. Also, the vice-versa is true where a vehicle will enter the Acceleration following regime from the Free Driving Regime if the Maximum Following Distance Threshold is passed.

The emergency regime occurs any time that the space headway is below the Minimum Following Distance Threshold. Equation 4-23 and Equation 4-24 calculate the acceleration in the Emergency regime. Equation 4-24 can be reduced to Equation 4-25 when individual drivers are considered.

$$b_n = \frac{1}{2}\frac{(\Delta v)^2}{ABX-(\Delta x-L_{n-1})} + b_{n-1} + b_{min} * \frac{ABX-(\Delta x-L_{n-1})}{BX} \quad \textbf{(4-23)}$$

$$b_{min} = -BMINadd - BMINmult * RND3_n + BMINmult * v_n \quad \textbf{(4-24)}$$

$BMINadd, BMINmult$ are calibration parameters

$RND3_n$ is a normally distributed driver dependent parameter

v_n is the speed of the subject vehicle

$$b_{min} = BMINadd + BMINmult * v_n \quad \textbf{(4-25)}$$

New Thresholds

Hook Following Threshold

The first and most prominent recurrent phenomenon in the naturalistic data is car following periods that begin at low space headways with the lead vehicle travelling at a higher speed than the subject vehicle. The low space headway and higher speed indicate the completion of a pass maneuver for the lead vehicle as it merges back into the same lane as the subject vehicle. The interesting phenomenon is that the completion of the pass maneuver initiates car following behavior. Table 4-1 shows that from a sample of the car following periods, this phenomenon represents 45% of the data which is too large to ignore.

Table 4-1: Random Sample Results for Number of Hook Following Periods

	Driver A	Driver B	Driver C	Driver D	% of Total
Regular Car Following	217	131	102	256	55%
Hook Car Following	166	123	142	149	45%

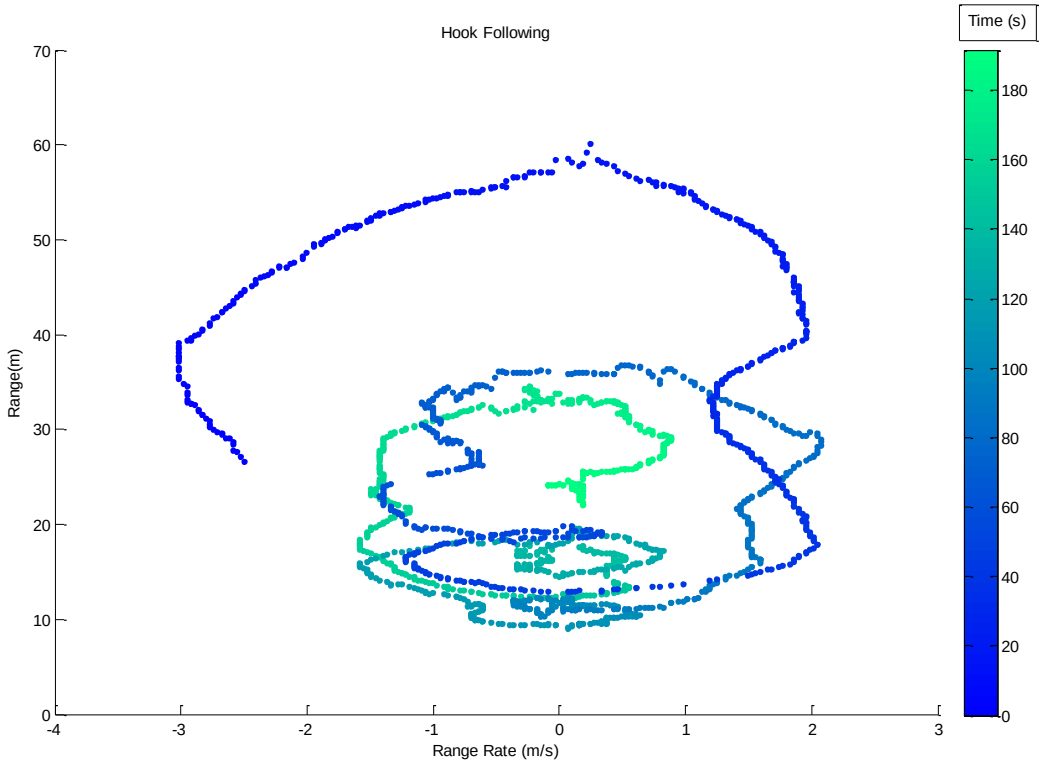

Figure 4-3: Example Hook Car Following Period

Figure 4-3 shows an example of hook car following behavior. It is deemed hook car-following because it is initiated by the subject vehicle "hooking" onto the faster lead vehicle. Figure 4-3 also shows that the vehicle moves into the unconscious reaction region and oscillates just like the regular Wiedemann model in Figure 4-1.

The process used was to plot two different sets of data and find the dividing line between them. The two data sets are one for vehicles that were not hooked onto for following and vehicles that were "hooked" onto and followed. The logic employed to differentiate between not hooking and hooking onto the lead vehicle operated upon the fact that if a car following period is initiated then the subject vehicle will travel faster than the lead vehicle in order to catch up and follow it.

Pass Threshold

The Wiedemann model uses an external lane change logic for pass decisions. Trends in the naturalistic data show that this pass decision could be represented by an n additional threshold to the Wiedemann model. This new threshold would operate much like the Perception Threshold, but the primary reaction would be to find a gap in an adjacent lane in order to pass. It will also operate like the Perception Threshold because the driver will need to react to the lead vehicle until an adequate gap is available.

The method employed here is the same as that employed for the Hook threshold except that the subject vehicle will decelerate in order to follow in this case.

4.5 Results

Evaluation of Existing Wiedemann Model

These new threshold equations were evaluated and calibrated using a genetic algorithm framework. The framework operated from state transitions where the driver would switch states when crossing a threshold. The progression of the states were as follows: Free Driving ->Approaching->Closely Approaching->Following Decelerate->Following Accelerate. The Emergency regime and Free Driving were not evaluated in order to focus on car following behavior. The evaluation consisted of 100 car following periods for four different drivers. The results of the genetic algorithm were compared to the VISSIM default values in Table 4-2. The length of the lead vehicle was evaluated as a calibration parameter in order to provide verification that the calibration is feasible. The results of the optimization function are shown in Table 4-3.

Table 4-2: Calibration Parameters by Driver

	Default	Driver A	Driver B	Driver C	Driver D
Ln-1	4.500	4.494	5.553	4.547	5.680
AXadd	2.500	2.525	5.044	2.873	5.601
BXmult	3.000	3.041	3.405	3.421	3.435
EXmult	2.500	2.514	3.096	3.427	2.676
CX	40.000	40.066	75.042	62.405	93.131
CX2	40.000	39.031	28.978	73.258	73.026
CLDVCX	30.000	31.762	56.798	33.159	51.080
OPDVmult	-2.250	-2.512	-6.580	-1.068	-3.307
bnull	0.100	0.122	0.075	0.241	0.072
bmaxmult	0.088	0.099	0.153	0.427	0.387
FaktorVmult	0.025	0.039	0.167	0.200	0.182
bminadd	-20.000	-20.898	-13.167	-23.408	-41.721
bminmult	0.025	0.033	0.091	0.320	0.378
Vdes	40.000	42.674	84.038	88.721	16.067
FaktorV	1.000	0.940	0.522	0.507	1.959

Table 4-3: Root Mean Square Error for Optimization Function

	Default	Calibrated	% change
Driver A	0.784762	0.7533074	4%
Driver B	4.016006	0.9688645	76%
Driver C	3.263291	1.2555831	62%
Driver D	17.55786	1.0745801	94%

The results show that Driver A behaves very similar to the VISSIM default values. The other drivers all show drastic improvement when calibrated. Also, a number of the parameters change drastically in value between drivers which suggests that drivers should be calibrated individually in order to preserve accuracy. The large variation also suggests that a generic model would be inaccurate.

New Thresholds

Hook Following Threshold

Figure 4-4 shows both the hooked and not hooked reactions. As can be seen in the figure, there appears to be a dividing line between two data sets. Figure 4-5 shows the same plot but with the dividing line. This same process is repeated for the other drivers and the equations are summarized by driver in Table 4-4.

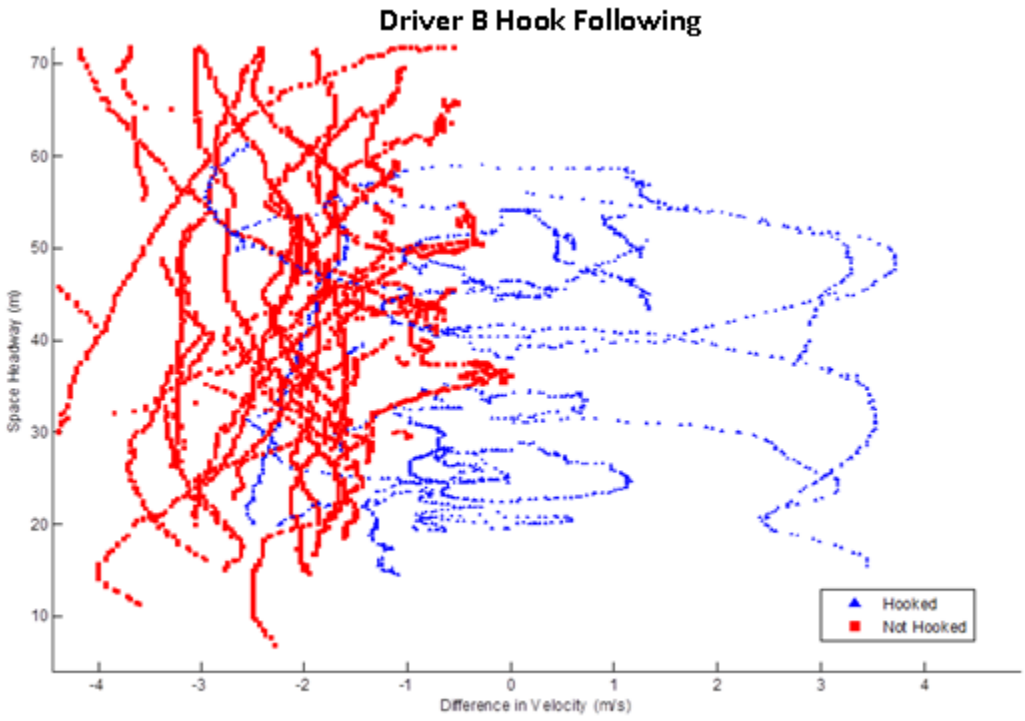

Figure 4-4: Hook/Not Hook Division (initial points on the left)

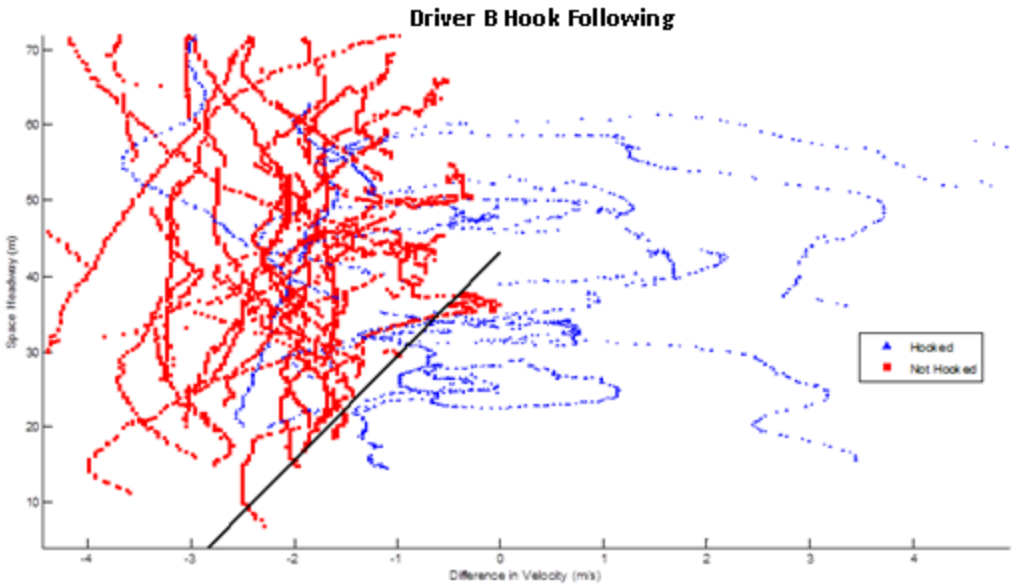

Figure 4-5: Hook/Not Hook Division Line

Table 4-4: Hook Following Threshold Equations by Driver

Driver	Threshold Equation
A	11.667*ΔV+49.667
B	13.822*ΔV+43.239
C	13.333*ΔV+46.5
D	15.789*ΔV+54.772

Pass Threshold

The pass threshold is harder to discern from than the hook threshold. Figure 4-6 shows data for Driver A which is unclear until forced following is considered. In forced following, the driver will intend to pass the lead vehicle, but there are not sufficient gaps in traffic in order to pass. When forced following is considered, the division between passing and not passing is clearly above any hard deceleration at low space headways.

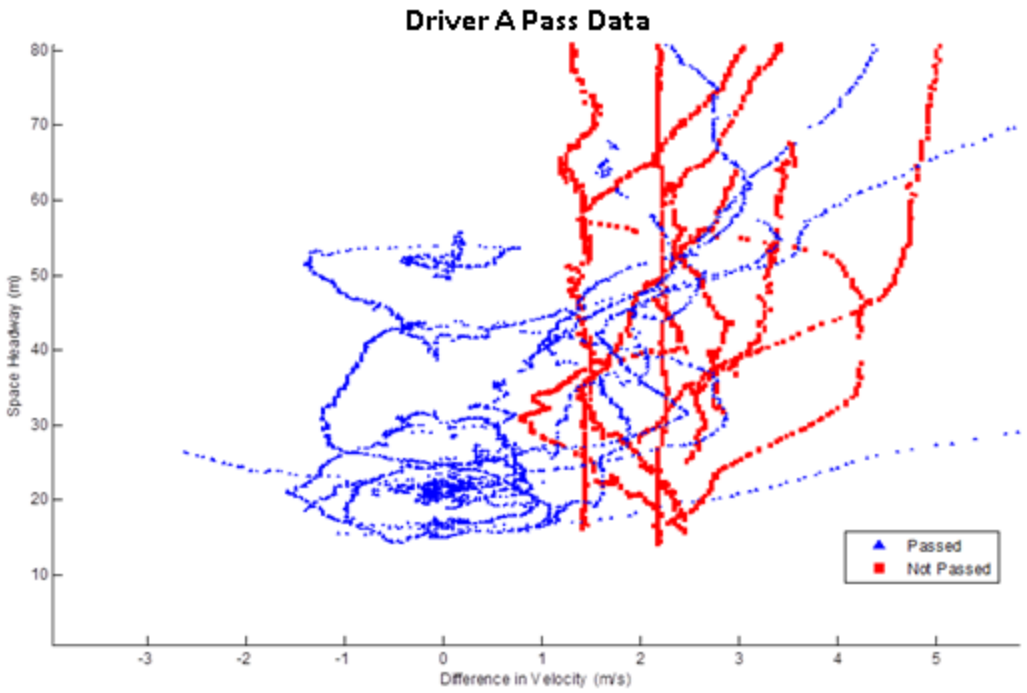

Figure 4-6: Pass/No Pass Data (initial points on the right)

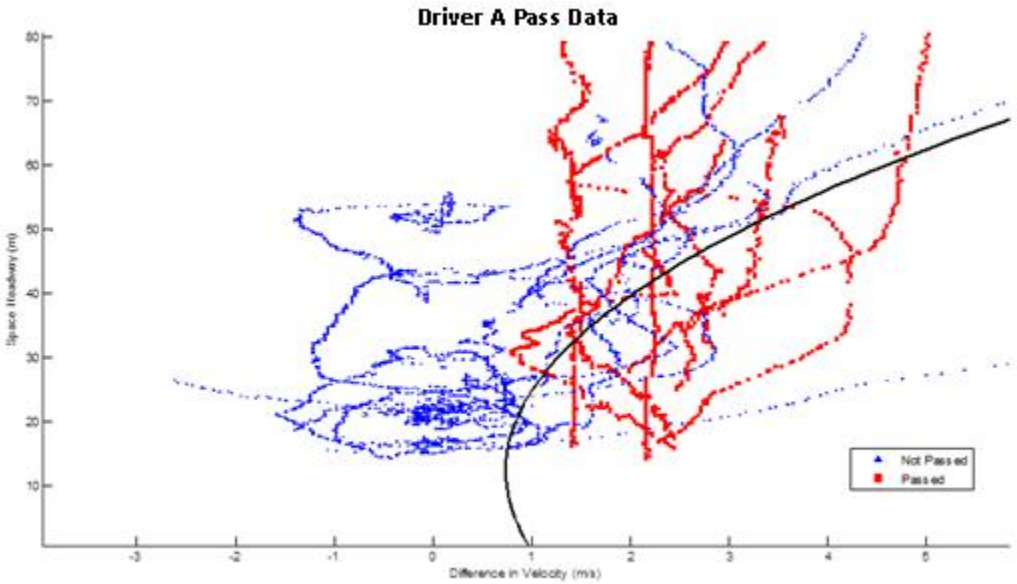

Figure 4-7: Pass Decision Curve

Table 4-5: Pass Threshold Equations by Driver

	Pass Threshold Equation
Driver A	0.0017Δx^2-0.0421Δx+0.9981
Driver B	0.0007Δx^2+0.0113Δx+1
Driver C	0.0017Δx^2-0.0672Δx+1
Driver D	0.0002Δx^2-0.0007Δx+1.5

Reconstructed Wiedemann Model

The calibrated parameters and new thresholds were calculated for each driver and are presented in Figure 4-8, Figure 4-9, Figure 4-10, and Figure 4-11. The SDV, Perception Threshold, and SDV2, Second Perception Threshold, are very similar for three of the drivers, but very different for Driver B. For Driver B, the CLDV or Closing Difference in Velocity threshold is greater than the Second Perception Threshold which means that Driver B prefers to decelerate at a harder rate when approaching a vehicle within the following regime. All of the drivers have Second Perception Thresholds that minimize the effect of the Acceleration following regime. The ABX, Minimum Following Distance, and SDX, Maximum Following Distance, Thresholds shows similarities between Drivers B and C, and Drivers A and D.

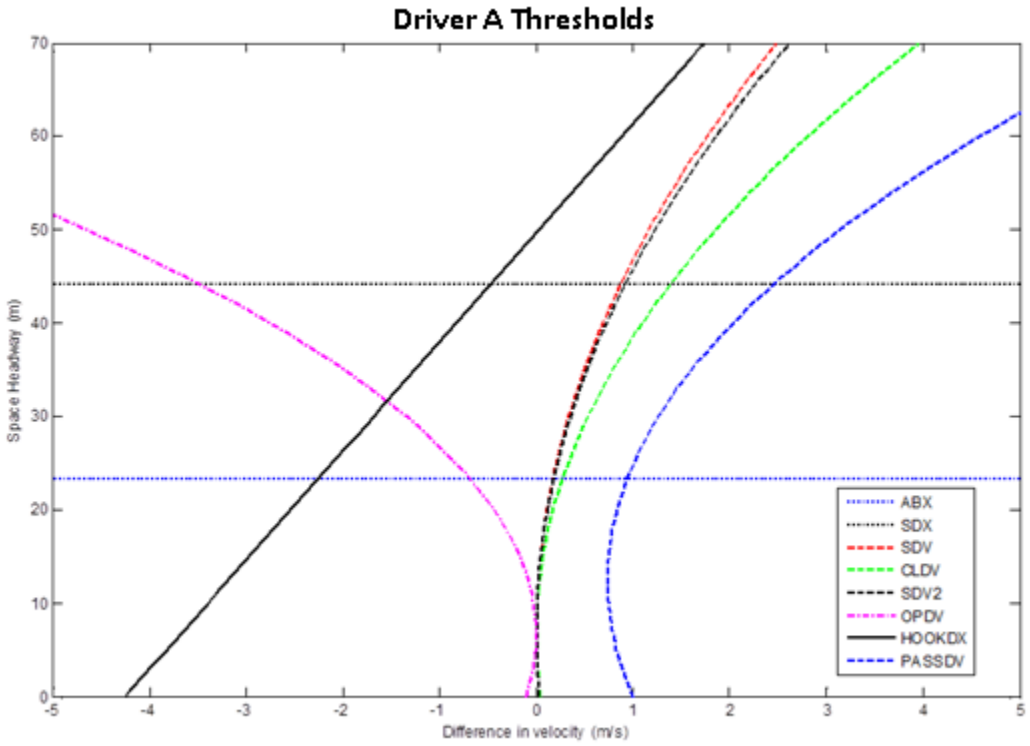

Figure 4-8: Thresholds for Driver A

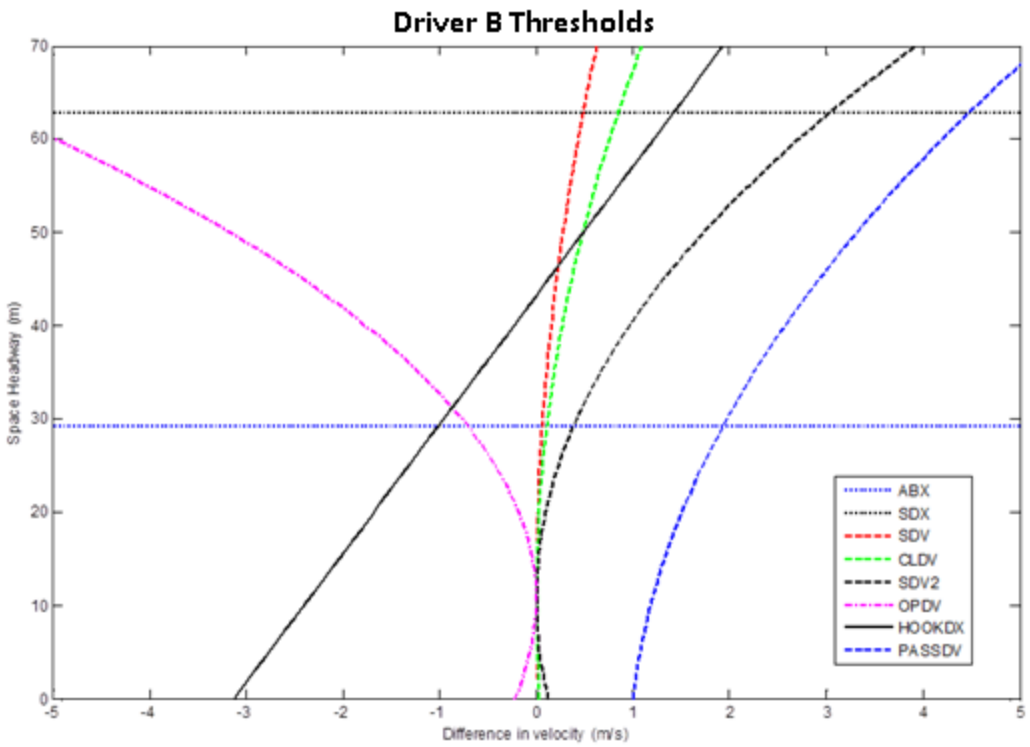

Figure 4-9: Thresholds for Driver B

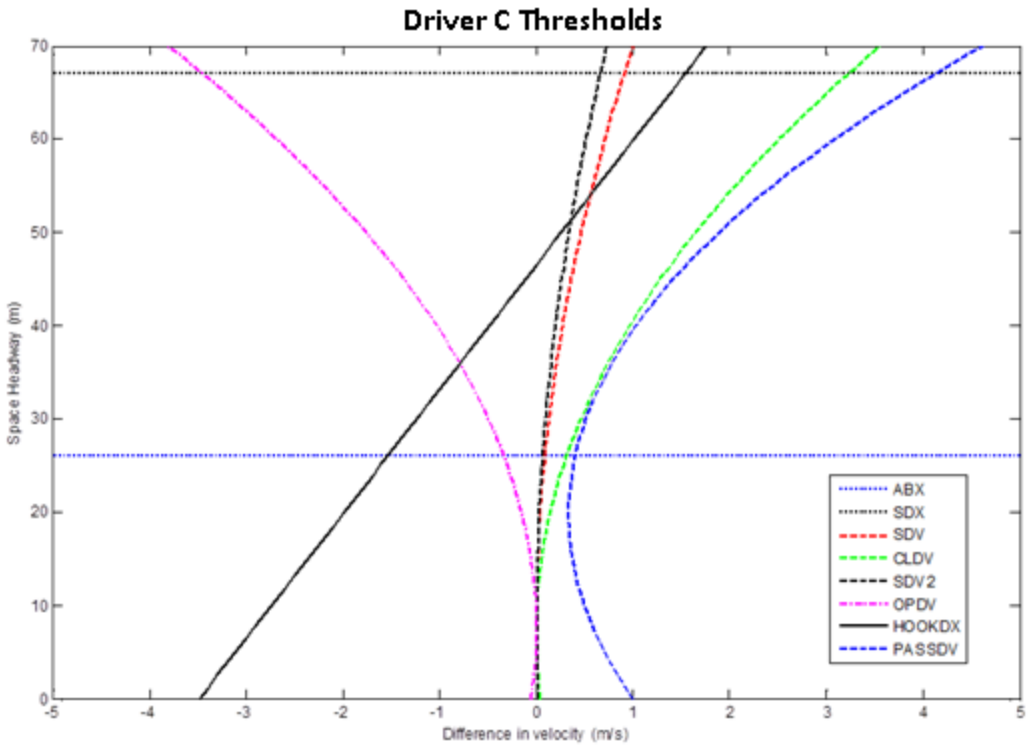

Figure 4-10: Thresholds for Driver C

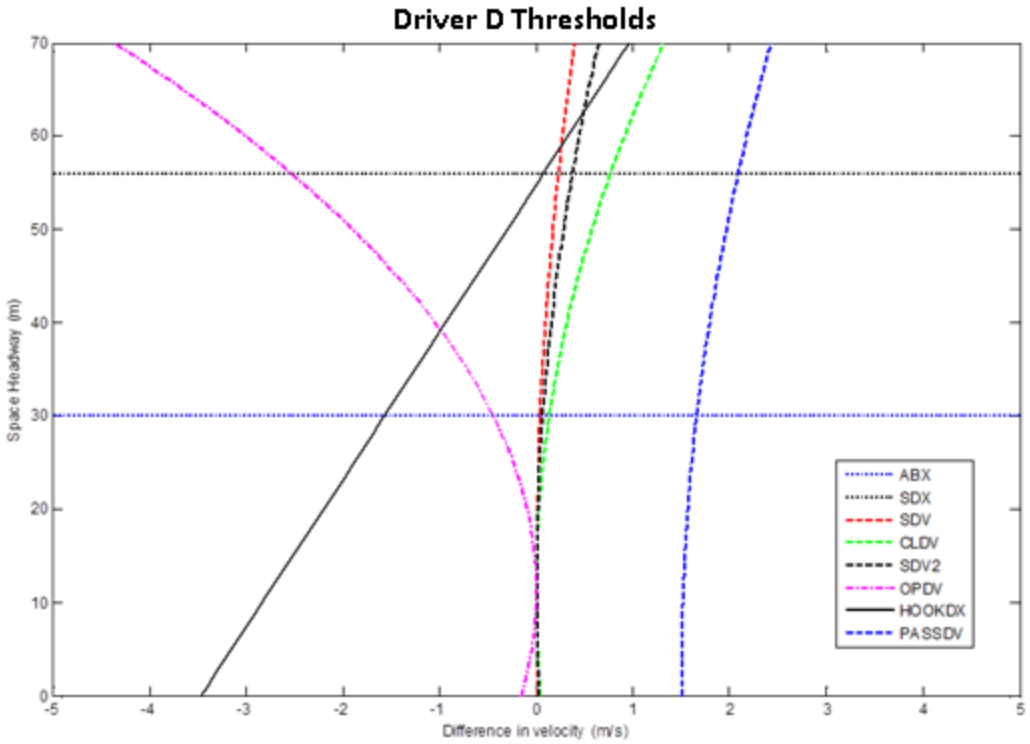

Figure 4-11: Thresholds for Driver D

4.6 Discussion and Conclusions

The method shown produces a new perspective to the Wiedemann model. This new perspective is to model and calibrate drivers individually in order to maintain accuracy. The inclusion of a hook following threshold adds value to the model by giving the model the ability to include a significant natural driving behavior. The addition of the pass threshold gives the model the ability to easily transition from car-following to lane change behavior. This threshold also provides a way to force car-following behavior when a lane change is not possible. The addition of these new thresholds and the driver specific equations all give the Wiedemann Model a better ability to represent "real world" driving behavior which is the goal of all car-following models.

References

AHMED, K. I. 1999. Modeling Drivers' Acceleration and Lane Changing Behavior. *PhD Dissertation*.

BRACKSTONE, M. 2003. Driver Psychological Types and Car Following:Is There a Correlation? Results of a Pilot Study.

HOOGENDOORN, S. & HOOGENDOORN, R. 2010. A Generic Calibration Framework for Joint Estimation of Car Following Models using Microscopic Data. *TRB 2010 Annual Meeting CD-ROM***,** 17.

KESTING, A. & TREIBER, M. 2008. Calibrating Car-Following Models using Trajectory Data: Methodological Study. 17.

MENNENI, S., SUN, C. P. D., P.E. & VORTISCH, P. 2008. An Integrated Microscopic and Macroscopic Calibration for Psycho-Physical Car Following Models *TRB 2009 Annual Meeting CD-ROM* 17.

OLSON, R., BOCANEGRA, R. J., HANOWSKI, R. & HICKMAN, J. 2009. DRIVER DISTRACTION IN COMMERCIAL VEHICLE OPERATIONS. Blacksburg VA: Center for Truck and Bus Safety

Virginia Tech Transportation Institute.

OSAKI, H. 1993. Reaction and anticipation in the Car-Following Behavior. *In Proceedings of the 12 International Symposium on the Theory of Traffic Flow and Transportation*.

OSSEN, S. & HOOGENDOORN, S. P. 2008. Validity of trajectory-based calibration approach of car-following models in presence of measurement errors. *Transportation Research Record***,** 117-125.

PANWAI, S. & DIA, H. 2005. Comparative evaluation of microscopic car-following behavior. *IEEE TRANSACTIONS ON INTELLIGENT TRANSPORTATION SYSTEMS*, 6**,** 314-325.

PTV-AG 2008. VISSIM 5.10 User Manual.

RANJITKAR, P. & NAKATSUJI, T. 2010. A TRAJECTORY BASED ANALYSIS OF DRIVERS' RESPONSE IN CAR FOLLOWING SITUATIONS. *TRB 2010 Annual Meeting CD-ROM***,** 21.

SCHULTZ, G. G. & RILETT, L. R. 2004. Analysis of Distribution and Calibration of Car-Following Sensitivity Parameters in Microscopic Traffic Simulation Models. 11.

SIUHI, S. & KASEKO, M. 2010. PARAMETRIC STUDY OF STIMULUS-RESPONSE BEHAVIOR FOR CAR-FOLLOWING MODELS. *TRB 2010 Annual Meeting CD-ROM*.

SUBRANMANIAN, H. 1996. Estimation of Car-Following Models. *Master Thesis*.

TOLEDO, T. 2003. Integrating Driving Behavior. *PhD Dissertation,*.

WIEDEMANN, R. 1974. Simulation des Strassenverkehrsflusses.

5. A HYBRID WIEDEMANN-GHR MODEL CALIBRATION USING NATURALISTIC DRIVING DATA[4]

Abstract

This research effort combines the Wiedemann car-following model with the GHR car-following model for trucks using The Naturalistic Truck Driving Study's (NTDS) data collected by the Virginia Tech Transportation Institute (VTTI). From past research efforts, it can be seen that the GHR model calibrates differently depending upon the situations that drivers face. The Wiedemann model uses thresholds in order to divide car-following into different regimes. These regimes represent different situations which correspond to a particular action to be taken. When the two models are combined, the Wiedemann model defines the different regimes while the GHR model calculates the accelerations based on those regimes. In this way, the two models work together in order to clarify the intended action of the driver as a result of different situations. The results of this combination along with the Naturalistic Data of four drivers show a difference in behavior between drivers and presents a measure of the attentiveness of different drivers. The results, in comparison to the Wiedemann model alone, show large improvement for two of the drivers and little improvement for the other two drivers.

[4] Paper has been published in the proceedings of the 13th International IEEE Annual Conference on Intelligent Transportation Systems

5.1 Introduction

In the last 50 years, a considerable amount of research has focused on modeling longitudinal driver behavior, producing a large number of car-following models including: Gazis-Herman-Rothery (GHR) models, safety distance models, linear models and psycho-physical or action point models. Calibrating these car-following models requires different levels of effort and the results are dependent upon data availability and the calibration method.

Several studies have tried to incorporate driver behavior or to classify driver's attributes, however, direct correlation with real driving variables is rare and parameterization of objective behavior is still in its development. Some studies have been limited to very controlled experiments while recent ones have used aerial photographs based on measurement from helicopters[1], GPS data [2][1], test track data and trajectory data from NGSIM [3][4].

Siuhi and Kaseko [5] demonstrated the need for separate models for acceleration and deceleration responses by developing a family of car-following models and addressing the shortcomings of the GM model. Previous work from Osaki [6] and Subranmanian [7] modified the GM model separating the acceleration and deceleration responses. Ahmed [8], following some work from Subranmanian assumed non linearity in the stimulus term and introduced traffic density. Results from Ahmed [8] and Toledo [9] showed, against popular belief, that acceleration increases with speed but decreases with vehicle separation. Due to statistical insignificance, Ahmed and Toledo also removed speed from their deceleration models. Siuhi and Kasvo [5] addressed some of these shortcomings developing separate models, not only for acceleration and deceleration, but also for steady-state responses. The models consisted of acceleration and deceleration response sub-models. In 1958, a series of models were developed at the GM Research laboratory by Chandler et al [10], Herman and Potts [11] and Gazis et al [12, 13].

The Gazis, Herman and Rothery model, usually referred to as the GHR model or as the *general car following mode,* was introduced in 1961. Ossen and Hoogendoorn [14] studied the car-following behavior of individual drivers using vehicle trajectory data that were extracted from high-resolution digital images collected at high frequency from a helicopter. The three models that form the roots of the GHR-model were compared. When individual drivers were analyzed, one model outperformed the other, however, after the results for all drivers were combined, it was found that no one model consistently outperformed the other models.

The results showed that in 80 percent of the cases, a relationship between the relative speed, distance, the speed of the subject vehicle, and the acceleration of the subject vehicle, could be established. According to the authors, the main contribution of their paper is that considerable differences between the car-following behaviors of individual drivers could be identified and that different car-following models appear to be optimal based on the individual driver data.

Brackstone summarizes the results of research into calibrating the GHR model. The results show variance in the three calibration parameters of the model. This means that

the model would not be adequate for a generic use. The results also show that the calibrated parameters values are different for the different types of acceleration and deceleration [15].

In 1974, Wiedemann [16] introduced a car-following model that is based on the psycho-physical behavior. The model has been improved since then by Leutzbach [17] by introducing perceptual thresholds as minimum values of the stimulus. The concept of thresholds in the Wiedemann model captures the driver's alertness in small space headway and the lack of explicit car-following behavior with large headways. In addition, it allows the model to explain the oscillation phenomena observed in car-following behaviors. Menneni et al [18] presented a calibration methodology of the VISSIM Wiedemann car-following model based on integrated use of microscopic and macroscopic data using NGSIM relative distance vs. relative speed graphs were used for the microscopic calibration, specifically to determine the action points (it is important to notice that action points were not identical to perception threshold). Scatter and distribution of action points on relative distance versus relative velocity graphs also showed similarity in driver behavior between the two freeways.

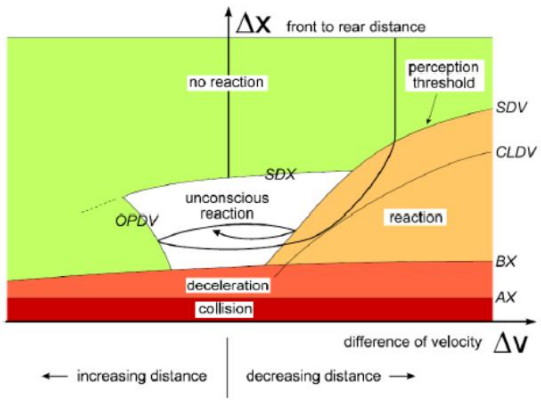

Figure 5-1: Wiedemann 74 Car Following Logic [19]

Figure 5-1 shows the graphical form of the Wiedemann 74 model. The different thresholds are shown with a certain shape that can only be amplified during the calibration procedure. The figure shows the subject vehicle approaching a lead vehicle (ΔX decreasing due to higher subject vehicle's speed shown by a positive ΔV), and entering a perception area (crossing the SDV threshold) where it has to reduce speed. The subject vehicle then crosses another threshold (CLDV) where it reacts and reduces speed even further to enter an unconscious reaction car-following episode. The subject vehicle then continues the unconscious car-following episode as long as it remains bounded by the OPDV, SDX, and SDV thresholds[16].

The Wiedemann model is threshold based with the thresholds defining different regimes. These regimes indicate different actions to be taken. The GHR model has only one regime for the decision of actions. The literature shows that the parameters of the GHR model vary based on the action, acceleration or deceleration. Combining these two models would present a framework where the Wiedemann model provides the logic for

the intended action of the driver while the GHR model calculates acceleration values based on that intended action.

5.2 Methodology

For this research, data from the VTTI Naturalistic Truck Driving Study was used. As opposed to traditional epidemiological and experimental / empirical approaches, this *in situ* process uses drivers who operate vehicles that have been equipped with specialized sensors along with processing and recording equipment. In effect, the vehicle becomes the data collection device. The drivers operate and interact with these vehicles during their normal driving routines while the data collection equipment is continuously recording numerous items of interest during the entire driving period. Naturalistic data collection methods require a sophisticated network of sensor, processing, and recording systems. This system provides a diverse collection of both on-road driving and driver (participant, non-driving) data, including measures such as driver input and performance (e.g., lane position, headway, etc.), four camera video views, and driver activity data. This information may be supplemented by subjective data, such as questionnaire data.

As part of the NTDS study [20], one hundred drivers were recruited from four different trucking fleets across seven terminals and one to three trucks at each trucking fleet were instrumented (nine trucks total). After a participant finished four consecutive weeks of data collection, another participant started driving the instrumented truck. Three forms of data were collected by the NTDS DAS: video, dynamic performance, and audio. Approximately 14,500 driving-data hours covering 735,000 miles traveled were collected. Nine trucks were instrumented with the DAS.

The following is a typical description of how the data collection is performed, along with accompanying screen shots and information describing how the system works and how data can be used. Four cameras monitor and record the driver's face, forward road view, and left- and right-side of the tractor trailer, which are used to observe the traffic actions of other vehicles around the vehicle. Figure 5-2 displays the four camera views and approximate fields-of-view. Low-level infrared lighting (not visible to the driver) illuminates the vehicle cab so the driver's face and hands could be viewed via the camera during nighttime driving. The sensor data associated with the project were originally collected in a proprietary binary file format. A database schema was devised and the necessary tables were created. The schema preserves the organization of data into modules; i.e., all of the variables associated with a particular module are stored in one table in the database. The import process itself consisted of reading the binary files, writing the data to intermediate comma separated value (CSV) files and "bulk inserting" the CSV files into the database. A stored procedure is available that allows one to query the database using the module and variable names rather than database table and column names.

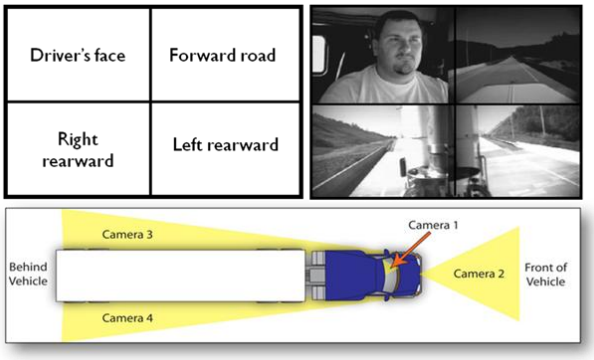

Figure 5-2: View of DAS data collection

Car-following situations were automatically extracted from the enormous volume of driving data in the database in order to analyze the car following driver behavior. The filtering process is an iterative process where initial values and conditions are used and after the events are flagged they are reviewed in the video data to adjust the values accordingly in order to obtain minimum noise. Visual inspection of the first subsets created revealed some non car-following events, so additional filtering was thus performed to remove these events from the database.

Specifically, car following periods were extracted automatically according to these conditions:

- Radar Target ID>0

  This eliminates the points in time without a radar target detected
- Radar Range<=120 meters

  This represents four seconds of headway at 70 mph
- -1.9 meters<Range*Sin (Azimuth) <1.9 meters

  This restricts the data to only one lane in front of the lead vehicle
- Speed>=20km/h

  This speed was used in order to minimize the effect of traffic jams, but still leave the influence of congestion in the data
- Rho-inverse <=1/610 meters^{-1}

This limits the curvature of the roadway such that vehicles are not misidentified as being in the same lane as the subject vehicle when roadway curvature is present.

- Length of car following period >= 30 seconds

The automatic extraction process was verified from a sample of events through video analysis. For the random sample of 400 periods, 392 were valid car following periods.

GHR Model

The GHR model is shown in Equation 5-1. The GHR model relates the acceleration to the current speed, relative speed, and space headway.

$$\boldsymbol{a_n(t) = cv_n^m(t)\frac{\Delta v(t-T)}{\Delta x^l(t-T)}} \quad (5\text{-}1)$$

$a_n(t)$ is the acceleration of the subject vehicle at time t

$v_n(t)$ is the speed of the subject vehicle at time t
T is the perception reaction time of the driver
$\Delta v(t-T)$ is the relative speed at time t minus T
$\Delta x(t-T)$ is the space headway at time t minus T
c, l, m are calibration parameters

Wiedemann Model Equations

The starting point for the Wiedemann model is the desired distance between stationary vehicles. The value calculated by Equation 5-2 is used in the calculations for the other thresholds.

$$\boldsymbol{AX = L_{n-1} + AXadd + RND1_n * AXmult} \quad (5\text{-}2)$$

L_{n-1} is the length of the lead vehicle
$AXadd, AXmult$ are calibrated parameters
$RND1_n$ is a normally distributed driver dependent parameter

The desired minimum following distance threshold is calculated using Equation 5-3 and Equation 5-4.

$$\boldsymbol{ABX = AX + BX} \quad (5\text{-}3)$$

$$\boldsymbol{BX = (BXadd + BXmult * RND1_n) * \sqrt{v}} \quad (5\text{-}4)$$

$BXadd, BXmult$ are calibration parameters
v is the minimum of the speed of the subject vehicle and the lead vehicle

The maximum following distance is calculated using Equation 5-5 and Equation 5-6. Equation 5-6 includes calibration parameters and random numbers, but mainly serves as a multiplier to BX.

$$\boldsymbol{SDX = AX + EX * BX} \quad (5\text{-}5)$$

$$\boldsymbol{EX = EXadd + EXmult * (NRND - RND2_n)} \quad (5\text{-}6)$$

$EXadd, EXmult$ are calibration parameters.
$NRND$ is a normally distributed random number.
$RND2_n$ is a normally distributed driver dependent parameter.

The Perception Threshold marks the point that a driver will begin to react to the lead vehicle. This threshold is calculated by the use of Equation 5-7. Equation 5-2 and Equation 5-8 are needed in order to calculate Equation 5-7.

$$\boldsymbol{SDV = \left(\frac{\Delta x - L_{n-1} - AX}{CX}\right)^2} \quad (5\text{-}7)$$

$$\boldsymbol{CX = CXconst * \left(CXadd + CXmult * (RND1_n + RND2_n)\right)} \quad (5\text{-}8)$$

L_{n-1} is the length of the lead vehicle. $CXconst, CXadd, CXmult$ are calibrated parameters. $RND1_n, RND2_n$ are normally distributed driver dependent parameters.

The reaction curve marks the location of a second acceleration change point while still closing on the lead vehicle. In VISSIM this threshold is assumed to be equivalent to the

Perception Threshold. Due to that similarity, the equation used for the Reaction Threshold, Equation 5-9 is derived from Equation 5-7.

$$\boldsymbol{CLDV} = \left(\frac{\Delta \boldsymbol{x} - \boldsymbol{L_{n-1}} - \boldsymbol{AX}}{\boldsymbol{CLDVCX}}\right)^{\boldsymbol{2}} \quad (5\text{-}9)$$

$CLDVCX$ is a calibrated parameter specific to one driver

The OPDV (Opening Difference in Velocity) curve is primarily a boundary to the unconscious reaction region. It represents the point where the driver notices that the distance between his or her vehicle and the lead vehicle is increasing over time. When this realization is made the driver will accelerate in order to maintain desired space headway. This threshold is calculated using Equation 5-10.

$$\boldsymbol{OPDV} = \boldsymbol{CLDV} * (-\boldsymbol{OPDVadd} - \boldsymbol{OPDVmult} * \boldsymbol{NRND}) \quad (5\text{-}10)$$

$OPDVadd, OPDVmult$ are calibrated parameters
$NRND$ is a normally distributed random parameter

The Wiedemann model reuses the Perception Threshold as a boundary to the unconscious reaction region. This would again be the point where the driver notices that the distance between his or her vehicle and the lead vehicle is decreasing over time, but this second use of the threshold is used when the subject vehicle is already engaged in following the lead vehicle. In our model, this reuse of the Perception Threshold was given its own equation in order to provide hysteresis control and to evaluate the adequacy of reusing the Perception threshold. Equation 5-11 is of the same form as Equation 5-7, but with a different calibrated parameter.

$$\boldsymbol{SDV2} = \left(\frac{\Delta \boldsymbol{x} - \boldsymbol{L_{n-1}} - \boldsymbol{AX}}{\boldsymbol{CX2}}\right)^{\boldsymbol{2}} \quad (5\text{-}11)$$

$CX2$ is a calibrated parameter

The first state is the free driving regime where the subject vehicle is not reacting to a lead vehicle and is travelling at a desired speed or accelerating to a desired speed. The Free Driving Regime is defined as the area above the Perception Threshold and the Maximum Following Distance Threshold. If the subject vehicle enters the free driving regime, the subject vehicle will then accelerate until the desired speed is reached. The value for this acceleration is calculated using Equation 5-12 and Equation 5-13. Equation 5-12 relates the maximum speed to the current speed times Equation 5-13 and calculates an acceleration value accordingly in order to reach the maximum speed. This regime was not included in the calibration because it would only complicate the evaluation of car following.

$$\boldsymbol{b_{max}} = \boldsymbol{BMAXmult} * (\boldsymbol{v_{max}} - \boldsymbol{v} * \boldsymbol{FaktorV}) \quad (5\text{-}12)$$

$BMAXmult$is a calibration parameter
$v_{max}$is the maximum speed of the vehicle

$$\boldsymbol{FaktorV} = \frac{\boldsymbol{v_{max}}}{\boldsymbol{v_{des}} + \boldsymbol{FAKTORVmult} * (\boldsymbol{v_{max}} - \boldsymbol{v_{des}})} \quad (5\text{-}13)$$

$FAKTORVmult$ is a calibration parameter
$v_{des}$is the desired speed

The approaching regime occurs when a vehicle in the Free Driving Regime passes the Perception Threshold. This vehicle will then decelerate according to Equation 5-14. The GHR model in Equation 5-1 replaces Equation 5-14. The GHR model, in this case, will have its own set of calibrated parameters specifically for approaching a lead vehicle.

$$\boldsymbol{b_n = \frac{1}{2}\frac{(\Delta v)^2}{ABX-(\Delta x - L_{n-1})} + b_{n-1}} \quad (5\text{-}14)$$

The Closely Approaching regime occurs only when a vehicle in the approaching regime passes the Closing Difference in Velocity Threshold. In VISSIM this regime is ignored, so the deceleration is still calculated by Equation 5-14. The Closely Approaching regime would typically result in a harder deceleration than the Approaching regime due to the low space headway. The GHR model accounts for this difference by using a specialized set of calibration parameters.

The Deceleration Following regime occurs as a result of a vehicle in the Approaching or Closely Approaching regime passing the Perception Threshold or a vehicle in the Acceleration Following Regime passing the Second Perception Threshold. When a vehicle enters the Deceleration Following regime the acceleration is calculated by the negative of Equation 5-15.

$$\boldsymbol{b_{null} = BNULLmult * (RND4_n + NRND)} \quad (5\text{-}15)$$

$BNULLmult$is a calibration parameter
$RND4_n$is a normally distributed driver dependent parameter

The Acceleration following regime occurs when a vehicle in the Deceleration Following regime passes the Opening Difference in Velocity Threshold or a vehicle in the Emergency Regime passes the Minimum Following Distance Threshold. The acceleration for a vehicle in the Acceleration Following regime is simply the positive value of Equation 5-15. If a vehicle in this regime accelerates and crosses the Maximum Following Distance Threshold, then that vehicle will enter the Free Driving regime. Also, the vice-versa is true where a vehicle will enter the Acceleration Following regime from the Free Driving Regime if the Maximum Following Distance Threshold is passed.

Equation 5-15 lacks any form of reaction to the lead vehicle. The only reaction is to switch from acceleration to deceleration once a threshold is crossed. This relies solely on the assumption that a constant small acceleration or deceleration will be sufficient to account for actions of the lead vehicle while in the following regime. The GHR model can be used to provide clarity in the two following regimes. The two regimes were calibrated with a different set of parameters in order to account and test for any difference between the accelerations and deceleration of the two following regimes.

The emergency regime occurs any time that the space headway is below the Minimum Following Distance Threshold. Equation 5-16 and Equation 5-17 calculate the acceleration in the Emergency regime. This regime is not included in the calibration because it resembles crash and near crash reactions more than car following.

$$b_n = \frac{1}{2}\frac{(\Delta)^2}{ABX-(\Delta x-L_{n-1})} + b_{n-1} + b_{min} * \frac{ABX-(\Delta x-L_{n-1})}{BX} \quad (5\text{-}16)$$

$$b_{min} = -BMINadd - BMINmult * RND3_n + BMINmult * v_n \quad (5\text{-}17)$$

$BMINadd, BMINmult$ are calibration parameters
$RND3_n$ is a normally distributed driver dependent parameter
$v_n$is the speed of the subject vehicle

Calibration Framework

The car following data for four different drivers from the Naturalistic Data was used to calibrate the models using a genetic algorithm. Ten car following periods per driver were used in the calibration. The framework consisted of calibrating the parameters for the Wiedemann model based on the equations shown earlier. This framework was then altered such that the GHR model replaced the acceleration equations in the following regimes: Approaching, Closely Approaching, Acceleration Following, and Deceleration Following. The GHR model was given a different set of calibration parameters (c,l,m,T) for each of those regimes. The reaction time, T, was used as a calibration parameter in order to obtain a measure of the attentiveness of the different drivers.

5.3 Results

Figure 5-3 shows how the Wiedemann model in its current state is very reactive to the changes in speed of the lead vehicle. This reactivity can be attributed to the fact that Equation 5-14 is a relative acceleration equation. Also, the recovery from a hard deceleration does not match the data in Figure 5-3.

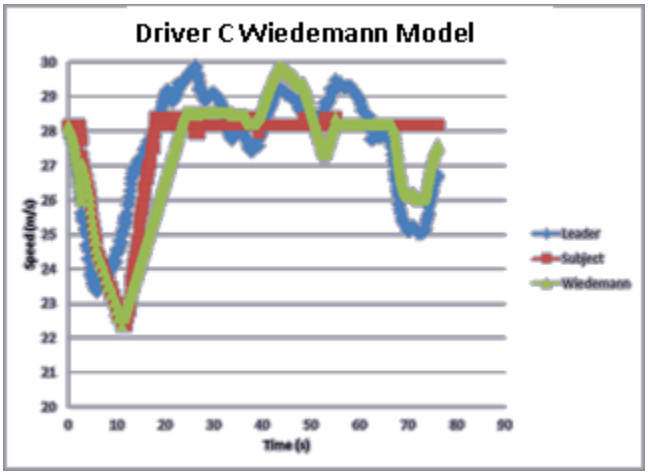

Figure 5-3: Driver C Wiedemann Car Following Period

Figure 5-4 presents the same car following episode as Figure 5-3, but with the GHR model integrated into the Wiedemann model. Figure 5-4 shows that the GHR model has removed the inaccurate reactivity to changes in the speed of the lead vehicle.

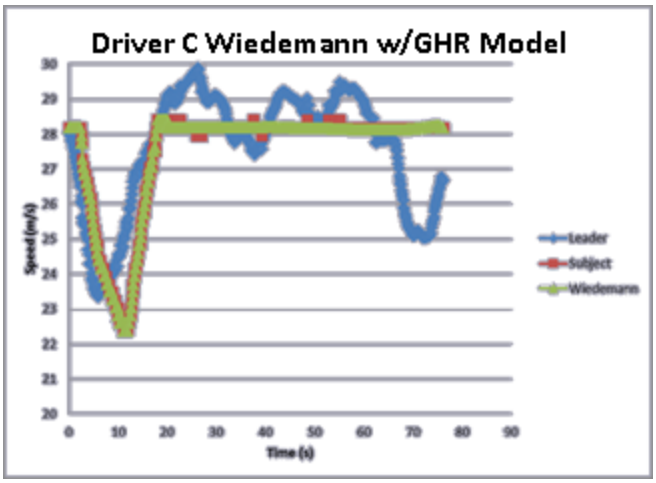

Figure 5-4: Driver C Wiedemann with GHR Car Following Period

Figure 5-5 is a comparison of the Wiedemann Model and the Wiedemann Model integrated with the GHR model. The GHR model corrects the recovery from a hard deceleration error seen in the Wiedemann model. The Wiedemann model appears to accelerate at a lower rate and for a longer period of time than the data.

Figure 5-5: Comparison of Wiedemann and Wiedemann with GHR

Figure 5-6 shows how the models compare in a Range vs. Range Rate graph. The Wiedemann model shows improper oscillation towards the end of the car following period. Also, the Wiedemann model remains in small oscillations at a high range when the data shows a larger oscillation moving to a smaller range at the end of the car following period.

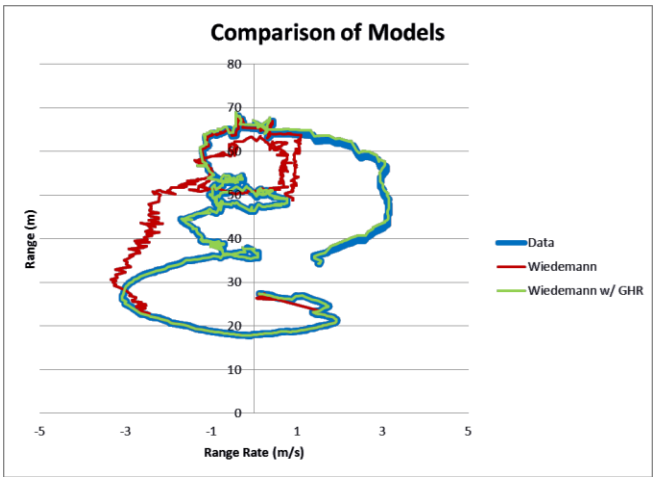

Figure 5-6: Comparison between Models in Range vs. Range Rate

Table 5-1 presents the results for the calibrated parameters of the GHR model by driver and regime. The values show variance between the drivers. The calibrated perception reaction times are low in some cases which indicate that in these cases the thresholds serve as decision points and actions from that point on are based on that decision. Low reaction time values in the following regimes (OPDV and SDV2) indicate more active and focused following behavior. High reaction times in the same region indicate more relaxed and inattentive following behavior. This is indicated by the fact that the stimulus for the reaction is either a change in relative speed or a change in the space headway.

Table 5-1: GHR Calibrated Parameters by Driver and Regime

	Driver A	Driver B	Driver C	Driver D
c SDV	0.064	0.935	0.446	0.434
m SDV	0.704	0.843	1.158	0.954
l SDV	2.135	1.997	2.046	1.933
T SDV	0.511	0.170	1.042	0.143
c SDV2	0.688	1.522	0.617	0.496
m SDV2	0.655	-0.592	0.734	0.337
l SDV2	2.613	2.565	1.821	2.002
T SDV2	0.227	0.511	0.498	0.505
c CLDV	0.130	0.532	0.602	0.706
m CLDV	0.880	-0.007	0.900	0.708
l CLDV	2.854	2.033	2.960	1.685
T CLDV	0.418	0.235	0.602	0.148
c OPDV	1.381	1.231	1.218	1.126
m OPDV	-0.521	-0.375	-0.064	-0.193
l OPDV	1.823	2.617	3.200	2.001
T OPDV	0.191	0.247	0.835	0.472

Table 5-2 presents the root mean square error values for both the Wiedemann model and the Wiedemann model integrated with the GHR model. The results show large improvement for two of the drivers, but little improvement for the other two drivers. This indicates that the Wiedemann model calibrates to two of the drivers better than the other two drivers. This means that the equations of the Wiedemann model reflect the behaviors of two of the drivers, but do not accurately reflect the behaviors of the other two drivers.

Table 5-2: Root Mean Square Error by Driver and Model

	Wiedemann	Wiedemann with GHR	% Improvement
Driver A	0.6684	0.6269	6%
Driver B	0.6042	0.4628	23%
Driver C	0.5980	0.3423	43%
Driver D	0.8106	0.7715	5%

5.4 Conclusions

The car following data for four different drivers from the Naturalistic Data was used to calibrate the models using a genetic algorithm. Ten car following periods per driver were used in the calibration. The framework consisted of calibrating the parameters for the Wiedemann model based on the equations for the thresholds and accelerations in the Wiedemann model. This framework was then altered such that the GHR model replaced the acceleration equations in the following regimes: Approaching, Closely Approaching, Acceleration Following, and Deceleration Following. The GHR model was given a different set of calibration parameters for each of those regimes. The reaction time, T, was used as a calibration parameter in order to obtain a measure of the attentiveness of the different drivers. The combination of the Wiedemann model and The GHR model present advantages when calibrating to the car following behaviors of individual drivers. The hybrid Wiedemann-GHR model calibrated to four individual drivers' results in 5-43 percent less error than the Wiedemann model alone. Future research should look into the transition between following and free-driving regimes and the driver actions in the emergency regime.

Acknowledgment

This material is based upon work supported by the Federal Highway Administration under Agreement No. DTFH61-09-H-00007. Any opinions, findings, and conclusions or recommendations expressed in this publication are those of the Author(s) and do not necessarily reflect the view of the Federal Highway Administration.

The authors would like to express thanks to individuals at Virginia Tech and the Virginia Tech Transportation Institute who contributed to the study in various ways: Greg Fitch, Shane McLaughlin, Zain Adam, Brian Daily, and Rebecca Olson.

References

[1] P. Ranjitkar and T. Nakatsuji, "A TRAJECTORY BASED ANALYSIS OF DRIVERS' RESPONSE IN CAR FOLLOWING SITUATIONS," *TRB 2010 Annual Meeting CD-ROM,* p. 21, 2010.

[2] W. Xin, *et al.*, "The less-than-perfect driver: A model of collision-inclusive car-following behavior," *Transportation Research Record,* pp. 126-137, 2008.

[3] S. H. Hamdar and H. S. Mahmassani, "Individual Variations versus Collective Traffic Patterns: Heterogeneity Effect in a Risk-Taking Environment," *TRB 2010 Annual Meeting CD-ROM,* p. 20, 2010.

[4] S. H. Hamdar and H. S. Mahmassani, "From existing accident-free car-following models to colliding vehicles exploration and assessment," *Transportation Research Record,* pp. 45-56, 2008.

[5] S. Siuhi and M. Kaseko, "PARAMETRIC STUDY OF STIMULUS-RESPONSE BEHAVIOR FOR CAR-FOLLOWING MODELS," *TRB 2010 Annual Meeting CD-ROM,* 2010.

[6] H. Osaki, "Reaction and anticipation in the Car-Following Behavior," *In Proceedings of the 12 International Symposium on the Theory of Traffic Flow and Transportation,* 1993.

[7] H. Subranmanian, "Estimation of Car-Following Models," *Master Thesis,* 1996.

[8] K. I. Ahmed, "Modeling Drivers' Acceleration and Lane Changing Behavior," *PhD Dissertation,* 1999.

[9] T. Toledo, "Integrating Driving Behavior," *Ph.D. Dissertation,,* 2003.

[10] R. E. Chandler, *et al.*, "Traffic Dynamics: Studies in Car Following," *Operations Research,* vol. 6, pp. 165-184, 1958.

[11] R. Herman and R. B. Potts, "Single lane traffic flow theory and experiment " *Proceedings of the Symposium on the Theory of Traffic Flow,* 1959.

[12] D. C. Gazis, *et al.*, "Car-Following Theory of Steady-State Traffic Flow," *Operations Research,* vol. 7, pp. 499-505, July 1, 1959 1959.

[13] D. C. Gazis, *et al.*, "Nonlinear Follow-The-Leader Models of Traffic Flow," *Operations Research,* vol. 9, pp. 545-567, 1961.

[14] S. Ossen and S. P. Hoogendoorn, "Validity of trajectory-based calibration approach of car-following models in presence of measurement errors," *Transportation Research Record,* pp. 117-125, 2008.

[15] M. Brackstone and M. McDonald, "Car-following: a historical review," *Transportation Research Part F: Traffic Psychology and Behaviour,* vol. 2, pp. 181-196, 1999.

[16] R. Wiedemann, "Simulation des Strassenverkehrsflusses," 1974.

[17] W. Leutzbach, "Introduction to the theory of traffic flow," 1988.

[18] S. Menneni, *et al.*, "An Integrated Microscopic and Macroscopic Calibration for Psycho-Physical Car Following Models " *TRB 2009 Annual Meeting CD-ROM* p. 17, 2008.

[19] PTV-AG, "VISSIM 5.10 User Manual," 2008.

[20] R. Olson, *et al.*, "DRIVER DISTRACTION IN COMMERCIAL VEHICLE OPERATIONS," Center for Truck and Bus Safety Virginia Tech Transportation Institute, Blacksburg VA FMCSA-RRR-09-042, 2009.

6. SUMMARY OF FINDINGS

6.1 Findings

Chapter 2 of this thesis focuses on comparing multiple car following models when calibrated to driver data from the Naturalistic Data. The results show that some of the microscopic traffic flow models calibrate to match the actual driver better than others. The results also show that some of the models are more adequate at mimicking different truck drivers. Most of the models show a behavior that is heavily influenced by the actions of the lead vehicle. The results of this research effort support that the Velocity Difference model and the Wiedemann model can adequately represent the behavior of different drivers. This means that if a single car following model is used with data from different drivers individually, these two models show the most promise in being up to the task. It is important to note that these findings are based solely upon data for truck drivers, so the applicability of these findings to car driver behavior would be questionable.

Chapter 3 of this thesis focuses on analyzing the Wiedemann model at different speeds. The results show that the thresholds of the Wiedemann model vary over the speed ranges. This variation seems to be dependent upon the driver and thus driver profiles should be used instead of a single parameter. The null acceleration also shows variance over the speed ranges that seem to be driver dependent. The OPDV and SDV2 thresholds show that the drivers are more responsive to approaching than falling behind a lead vehicle. The variances also show at which speeds each driver exhibits aggressive behavior which adds value to the model. The inclusion of different aggression behavior for different speeds will only improve the Wiedemann model and make it a more realistic mimicry of the real world. As far as simulation packages are concerned, the inclusion of the ability to change the parameters according to the speed of the vehicle would serve to increase the accuracy of simulations.

Chapter 4 of this thesis focuses on modifying the Wiedemann model to better match phenomenon and behaviors that appear in the Naturalistic Data. The method shown produces a new perspective to the Wiedemann model. This new perspective is to model and calibrate drivers individually in order to maintain accuracy. The inclusion of a hook following threshold adds value to the model by giving the model the ability to include a significant natural driving behavior. The addition of the pass threshold gives the model the ability to easily transition from car-following to lane change behavior. This threshold also provides a way to force car-following behavior when a lane change is not possible. The addition of these new thresholds and the driver specific equations all give the Wiedemann Model a better ability to represent “real world” driving behavior which is the goal of all car-following models.

Chapter 5 of this thesis focuses on combining the Wiedemann model with the GHR model in order to create a more accurate car following model. The car following data for four different drivers from the Naturalistic Data was used to calibrate the models using a genetic algorithm. Ten car following periods per driver were used in the calibration. The framework consisted of calibrating the parameters for the Wiedemann model based on

the equations for the thresholds and accelerations in the Wiedemann model. This framework was then altered such that the GHR model replaced the acceleration equations in the following regimes: Approaching, Closely Approaching, Acceleration Following, and Deceleration Following. The GHR model was given a different set of calibration parameters for each of those regimes. The reaction time, T, was used as a calibration parameter in order to obtain a measure of the attentiveness of the different drivers. The combination of the Wiedemann model and The GHR model present advantages when calibrating to the car following behaviors of individual drivers. The hybrid Wiedemann-GHR model calibrated to four individual drivers' results in 5-43 percent less error than the Wiedemann model alone.

6.2 Recommendations for Future Research

It is important to note that these findings are based solely upon data for truck drivers, so the applicability of these findings to car driver behavior would be questionable and thus would be recommended as an area of future research. Further research is also recommended in testing the Wiedemann model and Velocity Difference model with a larger number of individual drivers in order to clarify the strengths and weaknesses of each model. Future research is also recommended in the development and implementation of driver aggression profiles in the Wiedemann model. Also, discovering ways to group drivers according to their profiles would potentially reduce the number of profiles needed in order to gain a more accurate simulation of traffic flow. Future research should look into the transition between the following and free-driving regimes of the Wiedemann model and the driver actions in the emergency regime.